Relaxation Element Method in Mechanics of Deformable Solid

47

Ye. Ye. Deryugin, G. V. Lasko, and Siegfried Schmauder

Contents

Y. Y. Deryugin (✉)
Institute of Strength Physics and Materials Science, SB RAS, Tomsk, Russia
e-mail: dee@ispms.tsc.ru

G. V. Lasko · S. Schmauder
Institute for Materials Testing, Materials Science and Strength of Materials (IMWF), University of Stuttgart, Stuttgart, Germany
e-mail: Galina.Lasko@imwf.uni-stuttgart.de; Siegfried.Schmauder@imwf.uni-stuttgart.de

C.-H. Hsueh et al. (eds.), *Handbook of Mechanics of Materials*,
https://doi.org/10.1007/978-981-10-6884-3_30

Abstract

In this chapter a new method – the relaxation element method is justified. The definition of the changing of stress fields in solids under loading as a result of the change of elastic energy in a local volume, undergoing plastic deformation, is laid down at the basis of the method.

The Relaxation Element Method (REM) solves effectively two problems of a deforming solid (DS):

1. The construction of the different distributions of plastic deformation in local regions of various geometrical shape.
2. Modelling of the consequent involvement of separate structural elements into plastic deformation, operating on the principle of an inverse task of mechanics of deforming solids.

With this method a stress-strain state of the elastic plane with the sites of plastic deformation in the form of a circle, rectangle, and a localized shear band is analytically described. Examples of the construction of the sites of plastic deformation with gradients are given. The stress-strain state of a plane with a round inclusion is considered.

Examples of the simulations by the REM of the effects of Lüders band formation and interrupted flow in polycrystals are given. The analysis of the influence of rigidity of a testing device on qualitative and quantitative characteristics of the loading diagram is presented.

The effect of the gradients of plastic deformation on the stress of Lüders band initiation is analyzed. It is shown that the dependence of the stress of Lüders band initiation on grain sizes is the consequence of the independency of the gradient of plastic deformation under the changing of grain sizes.

A modified model of Griffith crack surrounded by a layer of plastically deformed material is proposed. Plastic deformation is shown to eliminate the singularity at the crack tip. The maximum stresses are observed at the boundary of the plastic zone in an elastically deformed matrix. The stress concentration increases as the thickness of the plastic layer decreases.

The obtained results testify to high predictable possibilities of the developed method. They are in a good agreement with known experimental data.

1 Introduction

The development of plastic deformation in the solid is known to proceed inhomogeneously in space and irregular in time. This property defines the process of plastic strain localization, developing in the course of loading of structurally

inhomogeneous materials. The evolution of nonhomogeneous distribution of plastic deformation is realized under the influence of various stress concentrators, caused by the inhomogeneity of the initial structure of the material and changing of stress state of the loaded system under prescribed boundary conditions. In the course of plastic deformation of local volumes, the continuous changing of the fields of internal stresses in the whole volume of the solid takes place. Technological and strength properties of the material depend on the character of the process of plastic strain localization and material degradation. In this connection there is an actual problem of the description and simulation of the process of plastic strain localization and changing of the stress-strain state of a structurally inhomogeneous medium with the site of plastic deformation under the different boundary conditions of loading. The description and simulation of these effects demand accounting for the multilevel character of the development of the processes in the deformed system, where the surface layer and internal interfaces affect the process of plastic deformation and fracture [1–4]. The evolution of an inhomogeneous distribution of plastic deformation is realized under the influence of different stress concentrators, and first of all under the influence of stress concentrators at the free surface of the solid. The pattern of macrolocalization of plastic deformation inherits the character of the distribution in the thin near-surface layer.

On the macrolevel one can select three types of macrolocalization of plastic deformation: Lüders band propagation, Portevin–Le Chatelier effect (PLC), and neck formation at the stage of prefracture [5–9]. For the description and simulation of the effect of intermittent flow, the relaxation element method (REM) developed by the present authors is suitable and promising [9–14].

The change in stress field in the solid under loading as a result of the decrease in elastic energy in the local volume, undergoing plastic deformation, lies on the basis of the method. Plastic deformation is the relaxation process in its nature. That means that in the site of plastic deformation a decrease in elastic energy takes place, i.e., the decreased level of stress is observed in comparison to the average stress level beyond the site of plastic deformation. For the fulfillment of this condition in the relaxation element method the notion of "relaxation tensor" is used, which characterizes a decrease in the field of elastic stresses in the given local volume as a result of its plastic deformation. The above approach allows solving effectively two problems of a deformed solid:

a) The description of the stress-strain state of the solid with the sites of different geometrical shape and with different distributions of the plastic deformation. Results are obtained using the known technique of continuum mechanics of a deformed solid and are represented in the form of analytical expressions for the components of the tensor of plastic deformation and stresses.
b) Simulation of the sequence of the involvement of separate structural elements into plastic deformation. Stress relaxation in local volumes changes the stress state in the whole volume of the solid. Thus, structural elements, having undergone plastic deformation in the surrounding of the elastically deformed matrix, play the role of the defect on a mesoscopic scale with its own field of internal stresses.

The presence of defects in a continuum is related to the existence of inhomogeneous stress fields in a volume of the material. Plastic deformation is the consequence of the collective movements of defects of different scale level. At the same time, the linear dependence of the components of the stress tensor breaks. There arises a fundamental problem of definition of the unambiguous connection between deformation and stresses. In the linear theory of elasticity, such a connection is represented by the generalized Hooke's law. In the continuum theory of defects [15, 16, 17], this obstacle is removed by the condition that the tensor of total deformation is equal to the sum of elastic ε_{ij}^{e} and plastic ε_{ij}^{p} deformation:

$$\varepsilon_{ij} = \varepsilon_{ij}^{e} + \varepsilon_{ij}^{p}. \tag{1}$$

The tensor of total deformation ε_{ij} is assumed to obey the compatibility condition. Thus, in the general case the tensors ε_{ij}^{e} and ε_{ij}^{p} could be incompatible. But the incompatibility of the tensor of elastic deformation is fully compensated by the incompatibility of the tensor of plastic deformation and vice versa. In particular, both ε_{ij}^{e} and ε_{ij}^{p} could be compatible. Then, the stress state of the medium will be exclusively defined by the tensor of elastic deformation ε_{ij}^{e}, connected with stresses through the generalized Hooke's law:

$$\sigma_{ij} = C_{ijkl}\varepsilon_{ij}^{e}. \tag{2}$$

Hence, according to the accepted assumptions, compatible plastic deformation cannot be connected with the stresses existing in the volume of a deforming solid. In other words, without additional conditions a compatible plastic deformation cannot be represented as an analytical function of the coordinates.

In the continuum theory of defects, a compatible and incompatible plastic deformation is calculated only in connection with the presence of the internal stress fields in each volume of the material.

Investigations show that the absolute majority of the defects at the stage of developed plastic deformation disappear as a result of annihilation, absorption at the sinks and interfaces, and the exposure at the external surface of the solid [18]. Together with deformation defects the stresses caused by the presence of the latter in the volume of the material disappear as well.

Traditional theories of plasticity take the macroscopic diagrams of work-hardening of real materials [19, 20, 21] into account, when defining the relation of the stresses in the local volume of a solid with plastic deformation in it, i.e., the integral (macroscopic) characteristics of mechanical properties are prescribed to the local volumes of the solid. Such an approach doesn't fully account for the relaxation nature of plastic deformation. On the other hand, continuum theories consider the field of plastic deformation in the local volumes of a solid in the form of defects with corresponding fields of internal stresses [15, 16, 17]. However, at that time, the problem of the connection of these fields

with the boundary conditions of loading of the solid and with the geometrical parameters of the initial microstructure of the material is not considered. In order to reveal this connection, let us consider the physics of the phenomenon.

According to the modern conception of physical mesomechanics [2–4], a physical reason of plastic flow in real materials is the mass transfer under the influence of an external applied stress. The creation and movement of dislocations occurs practically at the very beginning (onset) of loading, when due to the difference in elastic properties and anisotropy of structural constituents of the solid, the peak stresses (stress microconcentrators) arise in the volume of solid. Mass transfer causes continuous stress relaxation in the local volumes of the material. A different strain rate of plastic deformation in the local volumes results in its inhomogeneous distribution over the whole volume of a solid.

In many cases with a definite accuracy one can select a local volume, which undergoes plastic form changing. In such a case, one can state that plastic strain localization occurs. Very often such local volumes are called the sites or zones of plastic deformation, or the zones of plastic shearing. Experiments show that there are definite peculiarities of the formation of the zones of localized plastic deformation at each stage of loading [22–27]. A classical example is the Lüders band at the stage of its formation and propagation in polycrystals with highly pronounced yield stresses [28, 29].

The sources of movable deformation defects are, first of all, the free surface of the solid and various interfaces (grains, phases). Therefore, by prescribing the field of plastic deformation within these boundaries, we in principle take into account an initial structure of the material. Taking additionally into account the hierarchy of the structural levels of deformation [2–4], and the notions of physical mesomechanics, the site of plastic deformation should be considered as a volume defect of a higher scale level than microdefects such as dislocations and vacancies.

On this level, being commensurable with the elements of the initial structure (on mesolevel) bands of localized plastic deformation (LPD) form. On the background of a quasi-homogeneous distribution of plastic deformation, the bands of localized plastic deformation could be considered as defects of a corresponding mesoscale.

In polycrystals, for example, a single grain could be considered as a structural element of mesoscopic scale. The bands of localized plastic deformation can be considered as defects of a higher mesoscale if they embrace a conglomerate of grains. If the zone of localization spans over the region being commensurable with the width of the specimen, such a defect is necessary to be considered as a defect of macroscopic scale.

Below we consider the construction of the inhomogeneous distribution of plastic deformation on meso- and macrolevel, when the substitution of the real displacement field (with microscopic discontinuities from the movement of microdefects, such as dislocations) with the continuous one could be justified. This allows one to use fully the known methods of continuum mechanics when constructing an inhomogeneous distribution of plastic deformation in local regions and to calculate the corresponding stress concentrations in the solid at a definite scale level under prescribed boundary conditions of loading.

In this work, the relaxation element method (REM) is theoretically justified. This method allows one on the data of the sites of localized plastic deformation with a definite degree of accuracy to calculate the components of inhomogeneous stress fields caused by these sites. Besides that, in combination with other methods of analytical and numerical calculations of mechanics of deforming solid, this method allows by variation of structural, geometrical, and physical parameters to model the processes of the development of localized plastic deformation and at that time to check the validity of certain mechanisms of plastic deformation and fracture of real materials.

The idea of REM arose due to the authors' attempt to relate the change in plastic shape of a local volume of continuum with the value of stress drop or decrease in elastic energy in it. The phenomenon of elastic stress relaxation within the solids has long been known [30–33]. Its essence lies in the following: If a loaded sample is deformed up to a definite value, then at a fixed position of clamps the load will decrease in the process of time. The physical reason for stress relaxation, which is especially pronounced at elevated temperature, is the increase of the contribution of plastic deformation to the total deformation of the sample with time. Since the latter keeps constant, then with time the contribution of elastic deformation correspondingly decreases locally. A decrease in elastic deformation in the considered case is possible only under the decrease in applied stress in this volume. Analogous processes, apparently occur in local volumes of a solid, undergoing plastic flow. However, in literature the analysis of the correlation between physical processes, especially the process of plastic deformation and the value of relaxation within the local regions of a solid has received insufficient attention.

2 Relaxation Element Method

2.1 Relaxation Element as a Specific Defect in Continuum

Plastic deformation is the phenomenon of essentially relaxation nature. Hence, plastic (irreversible) form changing of the local volume in a loaded solid should be accompanied by stress relaxation in the given volume and arising of an inhomogeneous stress field in the whole volume of the solid. The process of formation of an inhomogeneous distribution of plastic deformation in continuum can be represented as a result of consequent chain of elementary acts of stress drop in the various local volumes of solid. Since the stress state of a solid is a tensor characteristic, then the value of stress relaxation in the local volume should be characterized by the tensor. In this connection, let us introduce the notion "relaxation element" (RE) as a specific defect in continuum. Tensor of relaxation $\Delta\sigma^r$ for such a defect should be unambiguously connected with the plastic formchanging of the local volume, i.e., inside this volume the field of plastic deformation, characterized by tensor $\Delta\varepsilon^p$, obeying the plastic displacement of the points at the external boundary of the given local volume should be assigned. Thus in general case, relaxation element is characterized by the geometrical shape of a local relaxation region and relaxation tensor $\Delta\sigma^r$, defining the field of internal stress outside and the field of plastic deformation $\Delta\varepsilon^p$ inside the given region.

One can imagine that in the process of loading in the volumes of a solid a number of elementary acts of stress relaxation in different local regions R_i occurs. By prescribing the distribution of the relaxation elements in the volume of material, we prescribe a definite distribution of plastic deformation, accumulated in the local volume in a definite time interval. One can imagine that in the process of loading in the volume of a solid a number of elementary acts of stress relaxation $d\sigma^{r_i}$ in different local volumes R_i occurs. By assigning a distribution of relaxation elements in the volume of a material, at that time we prescribe a definite distribution of plastic deformation, accumulated in the local volume in a definite time interval.

By summation of the fields from various RE just as for (as well as for) dislocations the superpositional principle is used since the elementary fields (from the elementary tensor of relaxation $d\sigma^{r_i}$) depend linearly on the corresponding boundary conditions of loading and on the boundary of region of relaxation R_i.

In other words, the characteristics of elementary fields depend linearly on the components of elementary tensor of relaxation $d\sigma^{r_i}$. It should be noted at that time, that the constancy of the loading conditions and the stress distribution at the external surface are assumed. A temporal sequence of the elementary acts of stress relaxation doesn't affect the integral result of the stress state of the solid.

2.2 Connection of Plastic Deformation with the Tensor of Stress Relaxation

The same relaxation tensor in principle can meet a variety of options of plastic strain distribution in the local areas of relaxation. In such a situation, a continuum theory suggests a most simple variant of the connection of tensor of relaxation with the tensor of plastic deformation. In principle, it is sufficient to solve the inverse problem: for the known field of internal stresses to define the tensor of plastic deformation in the local volume. Let us consider a simple example.

Shown in Fig. 1 is the scheme of tensile loading of the plane with the site of plastic deformation of arbitrary shape. Under the operation of external stress in a local region

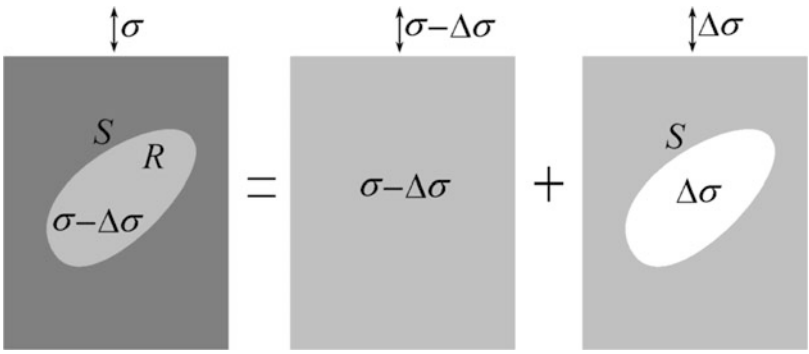

Fig. 1 Representation of a solution for the plane with the site of plastic deformation in the form of superposition of two solutions

S, a stress drop of the value $\Delta\sigma$ takes place. The general solution can be represented in the form of the algebraic sum of two solutions. The superposition principle is valid here because two solutions are summed up within an approximation of the linear theory of elasticity and the sum satisfies the required boundary conditions at the fields (places) of applied external stress and at the contour of the relaxation region. As it is seen, without a homogeneous field of stresses $\sigma - \Delta\sigma$ one can obtain the case of full stress relaxation within the regions of given configurations under external stress $\Delta\sigma$. The absence of stresses in the local region testifies to the fact that the formchanging of the local region R_i is characterized solely by the compatible tensor of plastic deformation $\Delta\varepsilon_{ij}^{p}$ [15, 16, 17]. In such a case, the continuity condition of the stress fields and field of plastic deformation are broken only at the boundary of this region, because tensors of elastic deformation ε_{ij}^{e} in the region R and stresses σ_{ij} beyond this region will be equal to zero. Let us emphasize once more that we consider only the final result but not the kinetics of stress relaxation.

A field of stresses fully determines an elastic deformation of the plane. Hence, beyond the region of relaxation, the deformation is fully defined. On the other hand, an inhomogeneous stress field beyond the relaxation region unambiguously defines the displacements of the points of the boundary of relaxation region, independently on the process of mass transfer inside the region of relaxation. The same displacements should be defined by the field of plastic deformation inside the local region of relaxation.

Therefore, from the many solutions for the tensor of plastic deformation, satisfying the given formchanging S, it is reasonable to choose the simplest linear one, obeying the equation $C_{ijmn}d\varepsilon_{mn,j}^{p} = 0$, as in the case of a boundary-value problem of the theory of elasticity with prescribed displacements. Thus, within this accepted approach, the plastic form changing of the local region we don't connect with the specific physical mechanism of plastic deformation. We are interested only in the stress state of the continuum.

At the boundary of the site of plastic deformation the compatibility condition of the tensor of plastic and elastic deformation is broken, as the stresses undergo discontinuity. At the same time, the sum of the tensor of elastic and plastic deformation satisfies the compatibility conditions everywhere.

Thus, from the standpoint of continuum theory of defects the value $\Delta\sigma^{r}$ and the geometrical shape of the local region of relaxation fully determine the stress-strain state of the plane and the distribution of plastic deformation in this region.

Let us emphasize that under the condition of full stress relaxation, the boundary conditions at the boundary of plastic regions are unambiguously related to the external applied stress. The changing of the load distribution at the external surface of a solid results in the corresponding changing of point displacements of the contour of ideal site of plastic deformation, i.e., boundary conditions at this contour, defining the tensor of plastic deformation inside this contour.

It is clear that there is no sense to speak about stress relaxation without the presence of a definite system of forces at the external surface of the solid, if suppose that there were no stresses in the solid before the testing. Disappearance of the elastic

field in a given volume is unambiguously connected with the arising of the field of plastic deformation. Thus, a physical law manifests itself explicitly, which points to the connection between the tensor of plastic deformation and stress relaxation tensor in the local region.

3 Stress-Strain State of the Continuum with the Site of Plastic Deformation

3.1 Examples of the Site of Plastic Deformation

Apparently, the stress state of the continuum with the site of plastic deformation depends on which components of stress tensor change as a result of relaxation, i.e., on the component of stress relaxation. However, in each case, a decrease in elastic energy in the site of plastic deformation will be accompanied by increase in stress beyond the site of plastic deformation.

As a simple example let us consider a stress state of the plane with the site of plastic deformation of round shape under the operation of external applied tensile stresses along the coordinate axis y. On a mesoscopic level in such an approximation one can imitate the influence of a separate grain of the polycrystal, undergone plastic deformation in surrounding of elastically deformed matrix.

For the simplification, let us consider the case of RE the tensor of relaxation of which is characterized by nonzero component $\Delta\sigma_y = \Delta\sigma$ directed along tensile axis y. That means that as a result of plastic deformation only the normal component of the tensor of stresses σ_y is relaxed.

The scheme of loading is represented in Fig. 2. The general solution (a) can be represented in the form of superposition of two separate solutions: homogeneous stress field: $\sigma - \Delta\sigma$ (b) and stress field for the plane under external tensile stress $\Delta\sigma$ (c), in the round region of which there exist no stresses. The last solution is known as Kirsch's problem for the plate with a round hole [34, 35].

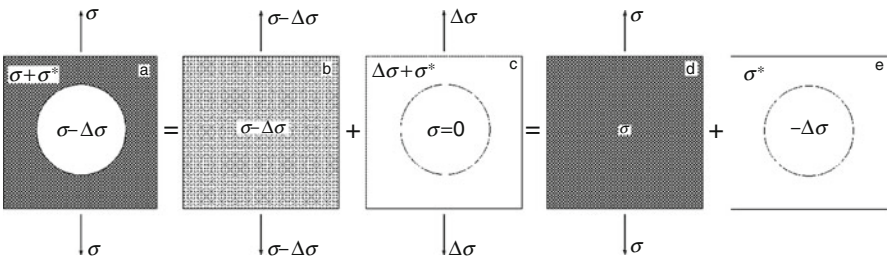

Fig. 2 Representation of the solution a in the form of superposition of simpler solutions: *1* – homogeneous stress field $\Delta\sigma - \sigma$ (b) and Kirsch's solution (c); *2* homogeneous field σ (d) and the field of internal stresses σ^* (e)

In the system of coordinates at the center of the circle and $0y$-axis along the tensile axis, beyond the site of plastic deformation, Kirsch's solution is characterized by the components:

$$\begin{aligned}
\Delta\sigma_y &= \frac{\Delta\sigma a^2}{2r^2}\left(3\left[1-\frac{2y^2}{r^2}\right]+\left(1-\frac{8y^2x^2}{r^4}\right)\left(\frac{3a^2}{r^2}-2\right)\right)+\sigma;\\
\Delta\sigma_x &= \frac{\Delta\sigma a^2}{2r^2}\left(\left[1-\frac{2y^2}{r^2}\right]-\left(1-\frac{8y^2x^2}{r^4}\right)\left(\frac{3a^2}{r^2}-2\right)\right);\\
\Delta\sigma_{xy} &= \frac{\Delta\sigma a^2 yx}{r^4}\left(3-\frac{2(3a^2+4y^2)}{r^2}+\frac{12a^2y^2}{r^4}\right).
\end{aligned} \tag{3}$$

Here $r^2 = x^2 + y^2$, σ – external tensile stress.

The considered example testifies to the fact that Kirsch's solution has a more deeper physical sense than the simple one as a stress in the plane with round hole. This solution defines also the fields of stresses beyond the sites of plastic deformation of round shape under the relaxation of stresses in it in a value $\Delta\sigma$. Theoretically one can imagine the case of full stress relaxation in a round region, i.e., when $\sigma = \Delta\sigma$ (Fig. 2c), then we obtain Kirsch's solution (3) in its pure form. As it is seen the absence of material in the local region doesn't mean the absence of material there. In our problem, the stress-strain state is caused by plastic deformation of the material in the local region of round shape and the region without stresses cannot be considered as a region where there is no material.

Since the plastic deformation is irreversible, then under unloading the plane will be elastically deformed. Therefore without homogeneous field of external stress σ (Fig. 2*d*), Kirsch's solution defines an inhomogeneous field of internal stresses in unloaded material σ^* (*e*), caused by the presence of the site of plastic deformation. Then inside the site the stress is equal to $\Delta\sigma_y = -\Delta\sigma$, i.e., the material is in the state of compression along the tensile axis till the value $-\Delta\sigma$.

Equation (1) without stresses $\Delta\sigma$ for the component $\Delta\sigma_y$ characterizes the field of internal stresses of a defect in the solid. Such a defect is the result of stress drop σ_y by the value $\Delta\sigma$ in a local volume of round shape. Shown in Fig. 3 are the patterns of spatial distributions of all the components of the fields of internal stresses σ^*. Maximum and minimum values of the component $\Delta\sigma_y$ are equal to $\Delta\sigma_{y\max} = 2\Delta\sigma$ and $\Delta\sigma_{y\min} = -\Delta\sigma$, respectively. As a result of stress relaxation inside the circle stress concentrations are observed at the boundary of the circle.

Let us characterize the field of plastic deformation in the site, corresponding to stress relaxation in the value $\Delta\sigma$ in the round region for the case of tension. This field ensures the full displacements of the points of the circle in Fig. 2c under the absence of the stresses in the site of plastic deformation. According to the solution of Kirsch's problem, the components of displacements of an arbitrary point (x_0, y_0) at the circle are equal:

$$u_y = 3y_0\Delta\sigma/E, \qquad u_x = -x_0\Delta\sigma/E. \tag{4}$$

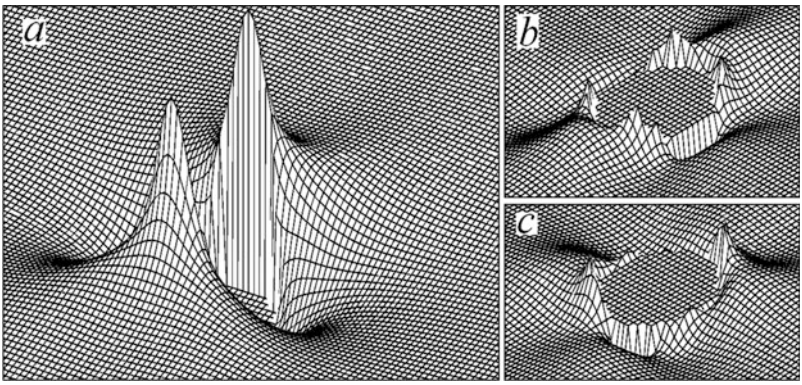

Fig. 3 Distribution of the components of the field of internal stresses σ^*: $\Delta\sigma_y(a)$, $\Delta\sigma_x(b)$, $\Delta\sigma_{xy}(c)$

The point displacements of the contour along the y-axis due to elastic deformation are equal to $u_y{}^{\mathrm{e}} = y_0\Delta\sigma/E$. Hence, the displacements due to plastic deformation are equal to $u_y{}^{\mathrm{p}} = 2y_0\Delta\sigma/E$ and $u_x{}^{\mathrm{p}} = -x_0\Delta\sigma/E$.

Thus, the field of plastic deformation should satisfy the following boundary conditions in displacements at the boundary of the contour:

$$u_y^{\mathrm{p}} = 2y\Delta\sigma/E, \qquad u_x^{\mathrm{p}} = -x\Delta\sigma/E. \tag{5}$$

The derivatives of the components of displacement field (5) over the corresponding coordinates define the components of the tensor of plastic deformation:

$$\varepsilon_y^{\mathrm{p}} = 2\Delta\sigma/E, \quad \varepsilon_x^{\mathrm{p}} = -\Delta\sigma/E, \quad \varepsilon_{xy}^{\mathrm{p}} = 0. \tag{6}$$

Under the operation of external stress $\Delta\sigma$ under the pure elastic deformation of plane (without plastic deformation), an elastic deformation will be observed inside the circle which is characterized by the components

$$\varepsilon_y^{\mathrm{e}} = \Delta\sigma/E, \quad \varepsilon_x^{\mathrm{e}} = -\nu\Delta\sigma/E, \quad \varepsilon_{xy}^{\mathrm{e}} = 0, \tag{7}$$

where ν – is the Poisson's ratio. Average values ν for solids in most cases lie within the range $\nu \approx 0.33$.

After stress relaxation in a $\Delta\sigma$-value, the elastic deformation of the circle decreases. This decrease is defined by the components represented by Eq. (7).

A comparison of (6) and (7) shows that plastic deformation not only compensates the disappeared contribution from elastic deformation, but makes additional contribution which two times exceeds the elastic deformation. Herewith, the region of relaxation increases along the y-axis and decreases along x-axis. Thus, the contribution of plastic deformation of the element to the changing of the shape of the circle

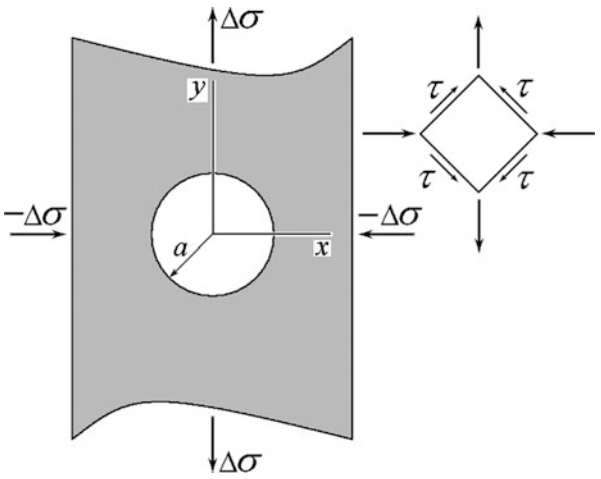

Fig. 4 The scheme for the calculation of stresses in the plane with a relaxation element of pure shear

two times exceeds the contribution of elastic deformation, disappeared as a result of stress relaxation.

At the boundary of the site, the components of the tensor of plastic deformation change jumplike from the value (6) down to zero, but the components of the tensor of elastic deformation from the value (7) up to (3) at the contour of the circle. Nevertheless, the displacements are not discontinuous when they transfer through the boundary of the site. A joint action of elastic and plastic deformation satisfies the continuity condition (compatibility) of the material at the boundary of the site of plastic deformation.

Let us consider another case, when stress relaxation occurs on the scheme of pure shear in conjugate directions at an angle of 45° with respect to the tensile axis (Fig. 4). Stress relaxation of pure shear can be realized by superposition of two separate solutions, correspondingly for the case of tension along the *y*-axis and for the case of compression along the *x*-axis (Fig. 4).

The case of tension is considered above and is described by Eq. (3). Analogically, an inhomogeneous stress field for the case of compression along the *x*-axis is defined. In the latter case, the same Eq. (3) are used where the stress $\Delta\sigma$ is taken with the opposite sign. Further in Eq. (3), the variable *x* will be exchanged into *y* and *y* into -*x*. The solution for the compression along *x*-axis will be obtained. Summing this solution with the solution (3), the following equations for the components of the stress tensor for the site of plastic deformation of pure shear will be obtained.

$$\begin{aligned}\Delta\sigma_y &= \frac{\Delta\sigma a^2}{r^2}\left(2\left[1-\frac{2y^2}{r^2}\right]+\left(1-\frac{8y^2x^2}{r^4}\right)\left(\frac{3a^2}{r^2}-2\right)\right),\\ \Delta\sigma_{xy} &= \frac{2\Delta\sigma a^2 xy}{r^4}\left(\frac{3a^2}{r^2}-1\right)\Delta\sigma_x = \frac{\Delta\sigma a^2}{r^2}\left(2\left[1-\frac{2y^2}{r^2}\right]-\left(1-\frac{8y^2x^2}{r^4}\right)\left(\frac{3a^2}{r^2}-2\right)\right).\end{aligned} \tag{8}$$

The patterns of spatial distribution of all the components of the field of internal stresses in the system of coordinates in Fig. 4 are shown in Fig. 5. The comparison

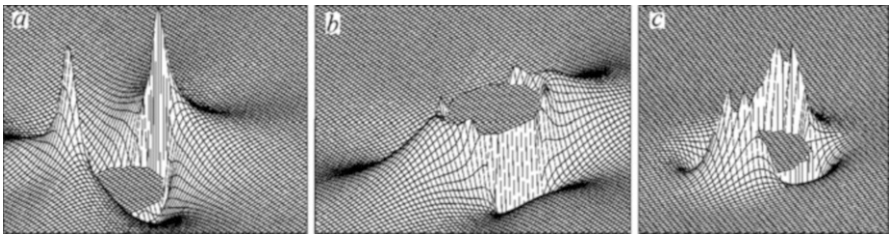

Fig. 5 Distributions of the components of the field of internal stresses of an RE of pure shear with respect to the system of coordinates in Fig. 4: $\Delta\sigma_y(a)$, $\Delta\sigma_x(b)$, $\Delta\sigma_{xy}(c)$

with Fig. 3 reveals qualitative and quantitative discripancies as well. Let us notice that here the maximum and minimum values of $\Delta\sigma_y$ components are equal to $\Delta\sigma_{y\max} = 3\Delta\sigma$ and $\Delta\sigma_{y\min} = -1.4\Delta\sigma$, respectively. The $\Delta\sigma_x$-distribution is the inverse distribution of the $\Delta\sigma_y$-distribution, which is rotated by 90° as well. Extreme values of the $\Delta\sigma_{xy}$-component are equal to $\pm 2\Delta\sigma$.

Inside the RE, there exists a homogeneous field of plastic deformation with the components:

$$\varepsilon_y^{\mathrm{p}} = 4\Delta\sigma/E, \varepsilon_x^{\mathrm{p}} = -4\Delta\sigma/E, \ \varepsilon_{xy}^{\mathrm{p}} = 0. \tag{9}$$

It is not difficult to define that the plastic deformation of pure shear in conjugate directions at an angle of 45° with respect to the tensile axis in the site is calculated according to the formulae

$$\gamma^{\mathrm{p}} = \left(\varepsilon_y^{\mathrm{p}} - \varepsilon_x^{\mathrm{p}}\right)/2 = 4\Delta\sigma/E. \tag{10}$$

At that time, in the direction at an angle of 45° with respect to tensile axis a shear stress is observed:

$$\tau\,(x, y) = \left(\Delta\sigma_y - \Delta\sigma_x\right)/2. \tag{11}$$

The equations obtained (8), (9), (10), and (11) above fully define the stress-strain state of the simplest site of plastic deformation of pure shear of round shape.

3.2 Construction of Relaxation Elements with Gradients of Plastic Deformation

The disadvantage of the considered distributions is the fact that at the boundary of RE the components of stresses and deformations possess jumps. And though formally the condition of compatibility for the total deformation (elastic + plastic) is obeyed the jumps of stresses mean loose of continuity of material along the boundary. The relaxation element method allows to construct and to find relaxation

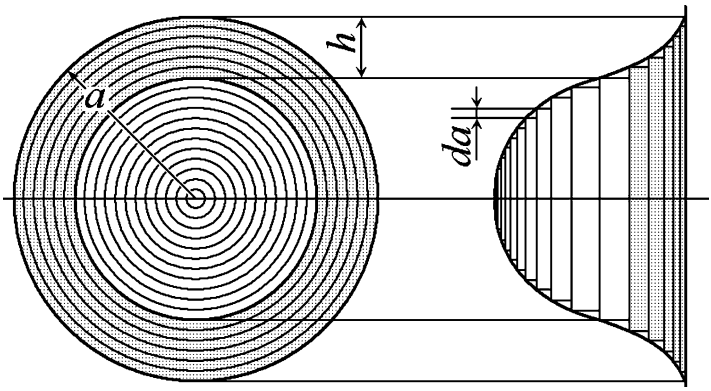

Fig. 6 The scheme of the family of RE and profile of plastic deformation in the family

elements with smooth distributions of plastic deformations. Let us demonstrate it with an example of RE of round shape.

By definition, the site of plastic deformation is the relaxation element is the defect in the continuum medium with its own fields of internal stresses. When $\Delta\sigma$ tends to a small value $d\sigma$, we obtain an elementary defect in the continuum. The presence of such a defect doesn't change the elastic properties of the medium, i.e., it doesn't affect the solution of the boundary-value problem of linear theory of elasticity. Therefore, for the internal fields of stresses of similar defect the superposition principle is valid. This defect can be used as the element for the construction of the various fields of localized plastic deformation. Prescribing a definite distribution of RE, one can construct the sites with the gradients of plastic deformation.

Let us consider it on the example of the site of plastic deformation of a-radius, constructed by superimposition of the RE of round shape on each other with the common center (Fig. 6). Each RE in the family is characterized by a definite dimension and the value of the elementary tensor of relaxation $d\sigma$. The boundaries of the neighboring elements are assumed to lie at the equal distance da from each other. Quantitative view (representation) of expected profile (smooth, differentiated) of plastic deformation is represented in Fig. 6 (to the right) in the form of envelope line, embracing the steps the height of which characterized the value of plastic deformation $d\varepsilon^{\mathrm{p}}$ of a definite RE. Let us select the near-boundary region with the width h in the given family of RE, in which parameters of RE will define in the following manner:

$$a(t'') = a - ht'', \quad d\sigma(t'') = (\beta + 1)h\,\Delta\sigma t''^{\beta} dt/a, \quad 0 \le t'' \le 1. \tag{12}$$

Here t'' is an integration variable, $\Delta\sigma$ is prescribed value, β – is the parameter, defining the value of elementary step when transfer from one element to another, $\beta + 1$ is normalization factor. It is seen that with increase in B t'' the dimension of RE evenly decreases from a till $a - t$. Herewith, the magnitude of the elementary relaxation tensor $d\sigma(t'')$ is gradually increasing. The growth rate depends on the value of the β-parameter. The more β, the more the growth rate of $d\sigma(t'')$.

Let the value of steps $d\varepsilon^{\mathrm{p}}$ in the central zone gradually decreases down to zero when approaching the center of the site. For that the changing of parameters of relaxation elements can be defined in the following manner.

$$a(t') = (a-h)(1-t'), d\sigma(t') = (\beta+1)(1-h/a)\,\Delta\sigma(1-t')^{\beta}dt, 0 \le t' \le 1. \tag{13}$$

Here t' – is the integration variable, which is changing within the interval $0 \le t' \le 1$, β – is the parameter, defining the change in the value of elementary stress drop $d\sigma(t')$. Accordingly (13), an increase in t' defines the gradual decrease in radius RE $a(t')$ and the value $d\sigma(t')$ as the center of the site is approached. The rate of reduction is controlled by the β-parameter. The higher is β-parameter, the quicker the value $d\sigma(t')$ decreases.

Using parameters (12) and (13) for the corresponding RE in Eqs. (8) and (10), we obtain the dependencies for the elementary stress field $d\sigma_i$ and plastic deformation $d\varepsilon_i^{\mathrm{p}}$ on the variables t' and t''. Integration of the elementary fields of plastic deformation from all RE under the prescribed conditions results in the smooth stress fields

$$\tau(x,y) = \Delta\sigma\left\{\begin{array}{l} \dfrac{(\beta+1)a^2}{(\beta+3)r^2}\left[\dfrac{3(\beta+3)a^2}{(\beta+5)r^2}-2\right]\left[1-8\left(1-y^2/r_2\right)y^2/r_2\right], \ \text{if} \ r^2 \ge a^2, \\ -1+\left(\frac{r}{a}\right)^{\beta+1}\left\{\dfrac{\beta^2-1}{2(\beta+3)(\beta+5)}\left[1-8\left(1-y^2/r_2\right)y^2/r_2\right]+1\right\}, \ \text{if} \ r^2 \le a^2 \end{array}\right\}. \tag{14}$$

and plastic deformation

$$\gamma^{\mathrm{p}} = \frac{2\Delta\sigma}{\mathrm{E}}\left\{\begin{array}{ll} \left(1-\dfrac{h}{a}\right)\left[1-\left(\frac{r}{a-h}\right)^{\beta+1}\right]+\dfrac{h}{a}, & r^2 \le (a-h)^2 \\ \dfrac{h}{a}\left(\dfrac{a-r}{h}\right)^{\beta+1}, & (a-h)^2 \le r^2 \le a^2. \end{array}\right. \tag{15}$$

Here r – is the distance from the center of the family of relaxation elements to the point with the coordinates (x, y).

To be short, Eq. (14) is written at the value $h = 0$. In Eq. (15), the upper equation behind the bracket defines the value of γ^{p}-component at each point of central zone (Fig. 6), and lower at each point in the near-boundary zone.

Apparently by pointed out method one can construct the smooth fields of plastic deformation and stresses for each RE of any type.

A smooth distribution of plastic deformation of pure shear at the value $\beta = 5$ is depicted in Fig. 7a. The profiles of plastic deformation for the different values of β-parameter are represented in Fig. 7b. At a distance h from the boundary of the site, the maximum gradient of plastic deformation is observed

$$\mathrm{grad}\varepsilon_y^{\mathrm{p}} = 2\Delta\sigma(\beta+1)/Ea. \tag{16}$$

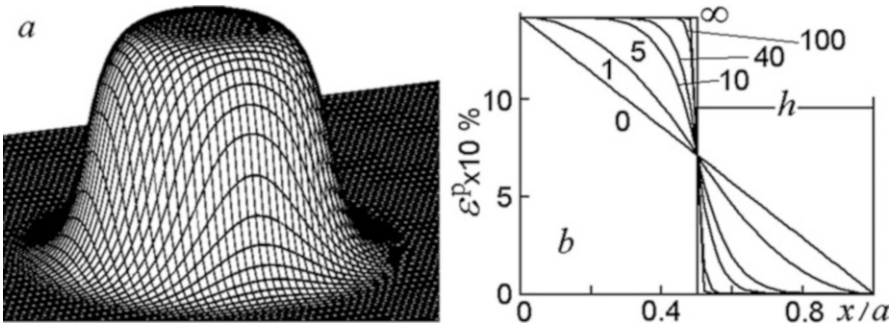

Fig. 7 Distribution (*a*) and profiles (*b*) of plastic deformation in the site at $h = 0.5a$ and $\beta = 5$. Numbers at the curves mean β-values

It is seen that the value of the gradient is defined by the parameter β. The more the value, the higher is the gradient of plastic deformation. At $\beta \to \infty$, we yield to the considered above the site of plastic deformation with the jump at the boundary of the site.

Shown in Fig. 8 are the parameters of the spatial distribution of plastic deformation and stress $\tau(x,y)$, for the various values of the parameter β at $h = 0.5a$. As the parameter β increases, the maximum gradients of plastic deformation and stresses increase as well. The case considered above with the jump of plastic deformation (and stress) is the limit case at $\beta = \infty$.

Figure 9 demonstrates the stress field (*a*) and isolines of pure shear (*b*) of the site of plastic deformation of pure shear at the values $\beta = 8$ and $h = 0.2a$. It is seen that such a site causes elevated stresses of a mesoscopic scale in the direction of 45° with respect to the tensile axis.

4 Stresses in a Continuum with Band Structures

4.1 Introduction

The band of localized deformation defines an extended narrow region on the surface of the material, where the process of stress relaxation occurs intensively and the material undergone the formchanging, additional to elastic one. On microlevel this region is represented as a pack of slip traces. In monocrystals such packs are formed along the closed-packed planes of atoms, favorably oriented for easy slip and spans (intersect) over the whole cross section of the specimen [36–39]. In polycrystals, first of all the conjugate grains are involved into plastic deformation, in which the slip traces are favorably oriented for the realization of shear component of external stress. On mesolevel, the straight bands of localized plastic deformation are formed. As a rule, they are oriented along the planes of maximum shear stress with respect to

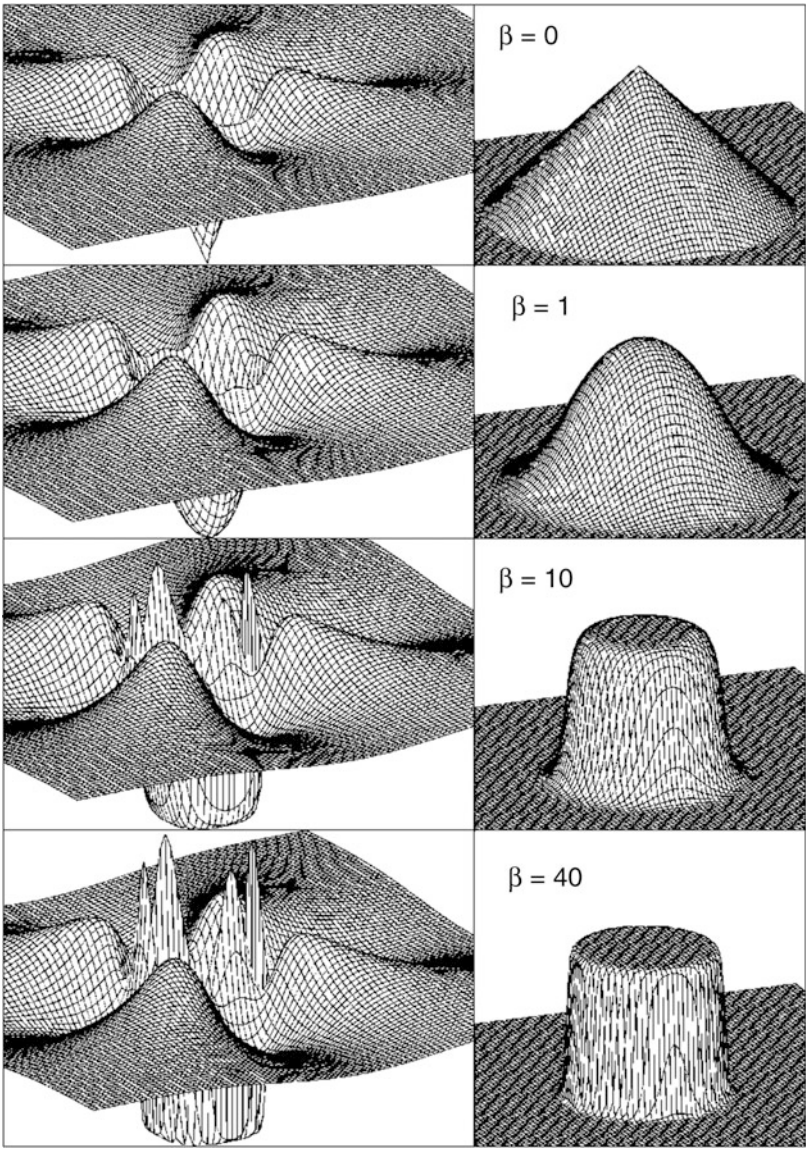

Fig. 8 Spatial distributions of stresses $\tau(x,y)$ (*a*) and plastic deformation of pure shear $\gamma^{p}(b)$, for different values of β-parameter

external applied stresses, independently on the crystallographic orientations of slip systems.

As experiment shows [38, 39] the phenomenon of material fragmentation on the mesolevel is, also, the consequence of the intersection and interaction of the forming mesobands, oriented at an angle of 45° or 60° with respect to tensile axis. On

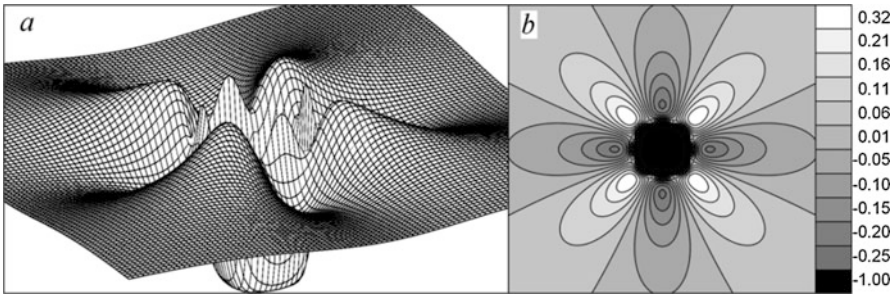

Fig. 9 Stress field (*a*) and isolines of RE of pure shear (*b*): $\beta = 8$, $h = 0.2a$

macrolevel they are incomplete Lüders band at the initial stage of loading, or band structures, being formed under the interaction of the macrobands of localized shear before the onset of fracture. In the case of the alloys with martensitic transformation inelastic formchanging of the local volumes takes place by formation or interaction of martensitic lamellae.

In such a manner, for the definition of the stress state of the medium with the band of localized deformation in the first approximation one should select the contours, beyond which the material deforms elastically, but inside undergoes plastic deformation, i.e. the plastic deformation is connected with stresses disappeared as a result of relaxation. Further, for convenience, under common term "Localized deformation" one should understand (mean) any inelastic deformation, obtained as a result of stress relaxation, independently on the physical mechanisms, providing inelastic form changing. Assigning (prescribing) in different manner the tensor of plastic deformation inside the contours, one can perform the analysis of the qualitative pattern of the change in the inhomogeneous field of stresses at the interaction of band defects at the mesoscale level.

In the given chapter provides the examples of construction of the bands of localized deformation with very different distribution of plastic deformation. It is shown how the field of stresses from corresponding distributions of RE are integrated. The stress-strain state of the band with localized plastic deformation, depending on the angle of its orientation with respect to tensile axis, is analyzed. Then, the interaction of the bands with each other and the edge effect are considered. The examples of the point displacement fields of continuum with the bands of localized deformation of different orientation and mutual location are considered. Qualitative and quantitative differences in the patterns of inhomogeneous stress field of fragmentated and non-fragmentated material are revealed.

4.2 Bands of Localized Plastic Deformation

One of the most interesting tasks practically and theoretically demanded in mechanics of deformed solid is the task of stress-strain state of the plane with the band of

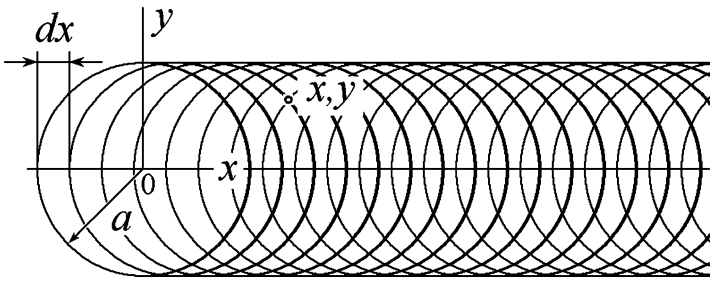

Fig. 10 The scheme of the construction of the band of localized deformation from RE of round shape

localized plastic deformation (LPD). Let us consider the simplest case of the construction of the band of localized plastic deformation, being normal to the tensile axis y. Let us compose it from the RE of round shape with the field of internal stresses (3). Let us define for each RE an elementary value of stress drop $d\sigma = \Delta\sigma dx/2a$, where $2a$ is the diameter of the circle and let us place the RE at the equal distance dx between each other along x-axis (Fig. 10). At such a construction in the arbitrary point (x,y), the stress drop will be equal to $nd\sigma$, where n–is the number of RE, inside which lies the given point. Stress drop in the value $d\sigma$, according to (6), is provided by elementary field of plastic deformation with the components

$$d\varepsilon_y^{\mathrm{p}} = 2d\sigma/E, \quad d\varepsilon_x^{\mathrm{p}} = -d\sigma/E, \quad d\varepsilon_{xy}^{\mathrm{p}} = 0. \tag{17}$$

Integrating these elementary fields (17), we obtain the following equations for the $\varepsilon_y^{\mathrm{p}}$-component of plastic deformation in hemi-infinite band:

$$\varepsilon_y^{\mathrm{p}} = \varepsilon_{y\max}^{\mathrm{p}} \begin{cases} \dfrac{x + \sqrt{a^2 - y^2}}{2a}, & x^2 + y^2 \le a^2; \\ \dfrac{\sqrt{a^2 - y^2}}{a}, & x^2 + y^2 \ge a^2. \end{cases} \tag{18}$$

Here $\varepsilon_{y\max}^{\mathrm{p}} = 2\Delta\sigma/E$.

The spatial distribution of the $\varepsilon_y^{\mathrm{p}}$-component of tensor of plastic deformation in the band is represented in Fig. 11. The maximum value of plastic deformation $\varepsilon_{y\max}^{\mathrm{p}}$ is observed along the axis of the band. As the boundary of plastic region is approached, the degree of plastic deformation decreases down to zero.

The same way, integrating elementary stress fields according to Eq. (3), where $\Delta\sigma$ is replaced by equation $d\sigma = \Delta\sigma dx/2a$, one can obtain the field of stresses for the given semi-infinite band of localized deformation. In a coordinate system with the origin at the 0-point (see Fig. 10), the components of the tensor of internal stresses of the given semi-infinite band are described by the simple formulas:

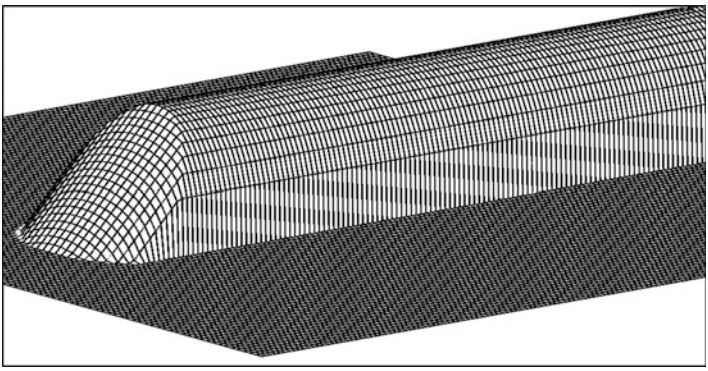

Fig. 11 Semi-infinite band of LPD

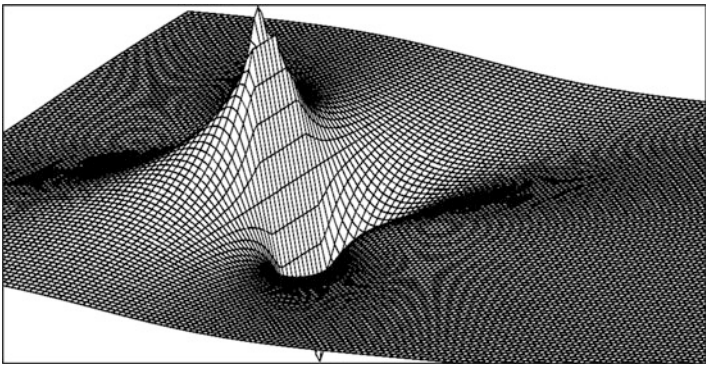

Fig. 12 Field of internal stress σ_y of semi-infi-nite LPD-band, being normal to tensile axis

$$\begin{aligned}
\Delta\sigma_y &= \Delta\sigma\begin{cases} \dfrac{ax}{r^2}\left(2+\left(1-\dfrac{a^2}{r^2}\right)\left(\dfrac{4y^2}{r^2}-1\right)\right), r^2 \geq a^2, \\ x/a, \quad r^2 \leq a^2 \end{cases} \\
\Delta\sigma_x &= \Delta\sigma\begin{cases} \dfrac{ax}{r^2}\left(2-\left(1-\dfrac{a^2}{r^2}\right)\left(\dfrac{4y^2}{r^2}-1\right)\right), r^2 \geq a^2, \\ \sqrt{1-y^2/a^2}, \quad r^2 \leq a^2 \end{cases} \\
\Delta\sigma_{xy} &= \Delta\sigma\begin{cases} \dfrac{ay}{r^2}\left(1-\dfrac{a^2}{r^2}\right)\left(3-\dfrac{4y^2}{r^2}\right), r^2 \geq a^2. \\ 0, \quad r^2 \leq a^2 \end{cases}
\end{aligned} \tag{19}$$

Shown in Fig. 12 is the distribution of the stress field σ_y (19). The stress field is seen to be perturbated only at the end of the band. There exists a stress concentration in front of the band. At that time the stresses are lower than the average level of external stress in the band itself, near the end. This example shows that the source of the driving force during the formation of the shearband is the concentration and high

gradients of stresses at the end of the band. One should take into account the following peculiarities of the bands of localized shear:

1. The stress field is highly perturbated only at the end of the band. There the stress concentration is observed always. It contributes to the formation of the LPD-band.
2. The zone of stress concentration at the end of the band is always combined with the zone of anticoncentration of stresses inside the band.

4.3 Plastic Deformation in the Site of Elliptical Shape

Let us consider an example of plane stress state of the medium, where the site of plastic deformation is described by the family of the elliptical regions of relaxation enclosed into each other (Fig. 13).

It is supposed that beyond a given site of plastic deformation, the material is homogeneous, isotropic and is deformed elastically under the operation of tensile stress σ, directed along y-axis. For definiteness let us assume that all ellipses have common center at the origin of coordinates. For the simplicity let us consider the case when the length of the semi-axes are equal to $a = a(1 - t)$ и $b = b(1 - t)$, i.e., when the ratio of the lengths of the semi-axes is the same and is equal to a/b, where the semi-axis b of the site is directed along the tensile y-axis, t – is the integration variable, changing within the interval from 0 to 1. At $t = 0$ we obtain the largest semi-axis. Hence an increase in t corresponds to the consequent transition from external contour to the center of the family. A specific t-value chooses a definite contour from the family. The point with the coordinates (x,y) will fit the contour of ellipses with the value $t = 1 - (x/a)^2 + (y/b)^2$.

The value of relaxation tensor for the given ellipse we represent in the form of the function of the integration variable in the following manner:

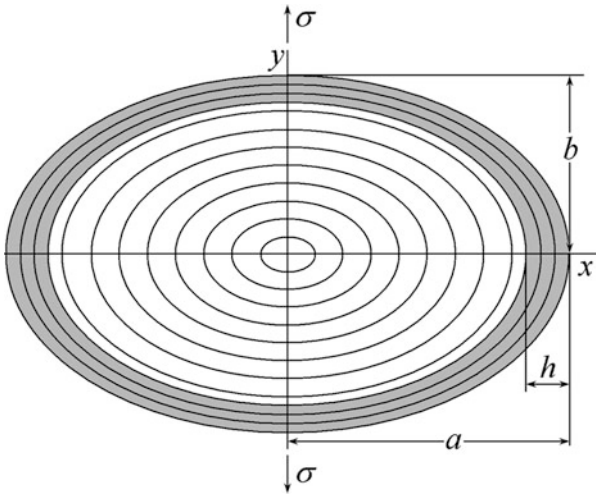

Fig. 13 Graphical representation of the distribution of the relaxation elements in the form of ellipses with the same relation of axis lengths

$$d\sigma^{r} = (\beta + 1)\sigma(1 - t)^{\beta} dt, \quad -1 \leq \beta \leq \infty. \tag{20}$$

The parameter β is seen to regulate the change in the value of relaxation under the continuous transition from the contour to contour. The coefficient $\beta + 1$ at the integration of $d\sigma^{r}$ from 0 to 1 determines the value of external applied stress σ.

One can show that the plastic displacements of the ellipse's contour as a result of stress drop inside the ellipse in the value $d\sigma^{r}$ are defined by the tensor of deformation with the components:

$$d\varepsilon_x = d\sigma^{r}/E_0, \quad d\varepsilon_y = (1 + 2a/b)\, d\sigma^{r}/E_0, \quad d\tau_{xy} = 0. \tag{21}$$

Apparently, the fields which covered the point (x,y) are superposed, i.e., the integral result is obtained by integration of the Eq. (21) within the limits $1 < t < 1 - \sqrt{(x/a)^2 + (y/b)^2}$.

By substituting into Eq. (21) instead of $d\sigma^{r}$ the Eq. (20) and integrating within the corresponding limits one can obtain the tensor components, describing the smooth field of plastic deformation with the gradients at the boundary of the site:

The distribution of the ε_y^{p}-component is characterized by simple equation

$$\varepsilon_y^{p} = \frac{\sigma}{E}\left(1 + 2\frac{a}{b}\right)\left[1 - \left(\frac{x^2}{a^2} + \frac{y^2}{b^2}\right)^{(\beta+1)/2}\right]. \tag{22}$$

In particular, along x-axis we obtain the following equation for the profile of plastic deformation

$$\varepsilon_y^{p} = \frac{\sigma}{E}\left(1 + 2\frac{a}{b}\right)\left[1 - \left(\frac{x}{a}\right)^{\beta+1}\right]. \tag{23}$$

An example of spatial distribution of plastic deformation for the different β-values according to Eq. (23) is represented in Fig. 14. As it is seen, this field is smooth. At the boundary of plastic region there is no breaks, only gradients of plastic deformation are broken. The maximum ε_y^{p}-value at the center of the site is not dependent on β-parameter and is equal

$$\varepsilon_{y\max}^{p} = \frac{\sigma}{E}\left(1 + 2\frac{a}{b}\right). \tag{24}$$

A derivative of the Eq. (22) on x variable results in the following equation for the gradient of plastic deformation along x-axis:

$$\mathrm{grad}\varepsilon_y^{p}(x) = -\varepsilon_{y\max}^{p}\frac{\beta + 1}{a}\left(\frac{x}{a}\right)^{\beta}.$$

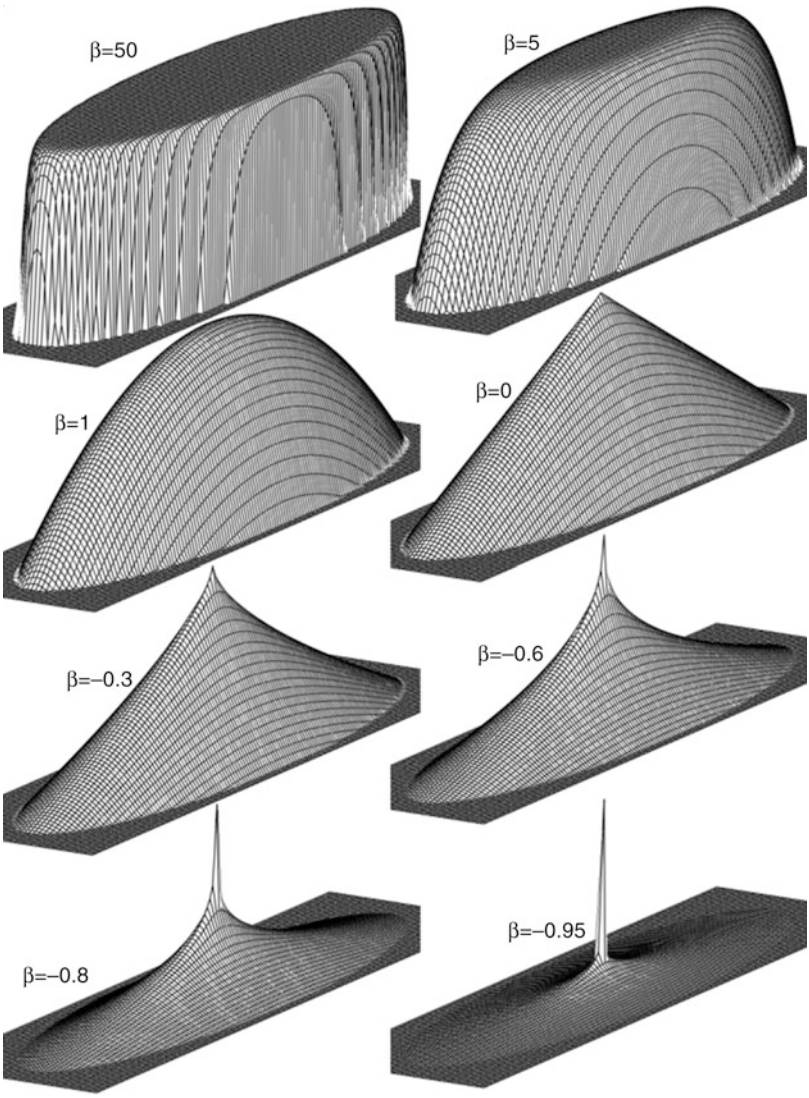

Fig. 14 The change in the distribution of plastic deformation ε_y in the site of elliptical shape with increase in β-parameter in Eq. (23); $a/b = 4$, $\sigma/E = 4.86 \times 10^{-3}$

At the end of the band a

$$\text{grad}\varepsilon_y^{\text{p}}(a) = -\varepsilon_{y\max}^{\text{p}} \frac{\beta + 1}{a}. \tag{25}$$

It is seen that with increase in β-parameter the gradients in front of the boundary increase. At the center of the site at $\beta > 1$, the gradient of plastic deformation is equal

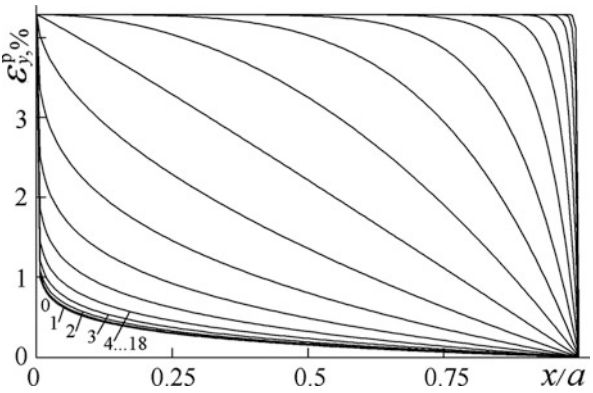

Fig. 15 The profiles of plastic deformation along x-axis when β increases according to Eq. (23)

to 0. At $\beta = 0$, the gradients along any directions from the center of the site are constant, i.e., plastic deformation decreases linearly from maximum value at the center down to zero at the boundary of plastic region. Then along x-axis $\text{grad}\varepsilon_y^p(x) = \varepsilon_{y\max}^p/a$.

At $\beta \to -1$ at the center of the site the gradient of plastic deformation tends to infinity. Figure 15 reflects all mentioned peculiarities on the profiles of plastic deformation ε_y^p along x-axis under increasing the value of β-parameter according to the law, $\beta = -0.95 + 2^{j-9}$, where j in order takes the numerical values from 0 till 18.

It is clear that the selection of another law for the relaxation value at the same distribution of relaxation elements will result into another distribution of plastic deformation. Shown in Fig. 15 is the analogous example, when the law for the value of relaxation is set by the equation

$$d\sigma^r = (\beta + 1)\sigma t^\beta dt, \; -1 \le \beta \le \infty. \tag{26}$$

Then the distribution of ε_y^p-component is defined by the equation

$$\varepsilon_y^p = \frac{\sigma}{E}\left(1 + 2\frac{a}{b}\right)\left[1 - \sqrt{\frac{x^2}{a^2} + \frac{y^2}{b^2}}\right]^{\beta+1}. \tag{27}$$

And for the profile of plastic deformation the following equation is obtained

$$\varepsilon_y^p = \frac{\sigma}{E}\left(1 + 2\frac{a}{b}\right)\left[1 - \frac{x}{a}\right]^{\beta+1}. \tag{28}$$

It is seen that, unlike the previous case, here, conversely, increase in β-parameter results in decrease in localization of plastic deformation. The peculiarity of the distribution of (28) lies in the fact that at $\beta > 0$ at the boundary of the site there is no jump of the gradient of plastic deformation (Fig. 16). It should be noted that the profiles in Fig. 16 exactly copy inversely reflected profiles in Fig. 15. Besides

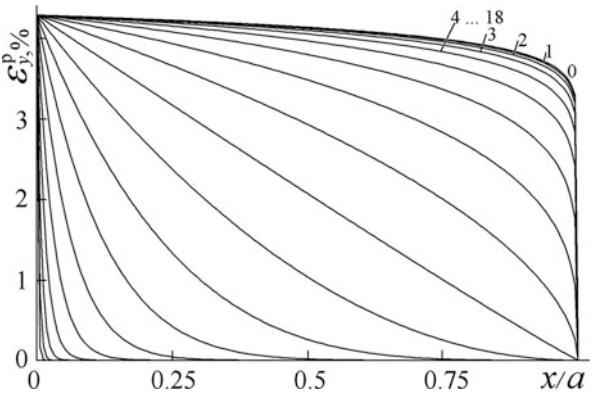

Fig. 16 The changing of the profiles of plastic deformation along x axis under increase in β according to Eq. (27)

that, maximum values ε_y^p at the prescribed values of relations a/b and σ/E don't depend on the β-value. In Figs. 15 and 16 the ratio $a/b = 4$, $\sigma/E = 4.86 \times 10^{-3}$, $\varepsilon_{ymax}^p = 4.43\%$.

By combination of solutions (23) and (27) one can obtain the distribution which will be smooth (differentiable) at all points of the site of plastic deformation including the boundary of the site. For this it is necessary for the RE in the near-boundary zone of the width h along x-axis (Fig. 13) to prescribe the relaxation law by the equation the type (20), and for the rest of relaxation elements in distribution – the Eq. (26), providing the matching of the gradients at the contour, separating the selected zones. Then the continuity condition of the gradients will be fulfilled everywhere and the distribution of plastic deformation will be described by the formulae:

$$\frac{\varepsilon_y^p}{\varepsilon_{ymax}^p} = \begin{cases} \left(1-\frac{h}{a}\right)\left[1-\left(\left(\frac{a}{a-h}\right)\sqrt{\frac{x^2}{a^2}+\frac{y^2}{b^2}}\right)^{\beta+1}\right]+\frac{h}{a}, \sqrt{\frac{x^2}{a^2}+\frac{y^2}{b^2}} \le 1-\frac{h}{a} \\ \frac{h}{a}\left[\left(1-\sqrt{\frac{x^2}{a^2}+\frac{y^2}{b^2}}\right)\frac{a}{h}\right]^{\beta+1}, 1-\frac{a}{h} \le \sqrt{\frac{x^2}{a^2}+\frac{y^2}{b^2}} \le 1. \end{cases} \quad (29)$$

The result at $h/a = 0.5$ and for the rparameters of ellipse is represented in Fig. 17.

As should be expected, distribution of plastic deformation is turned out to be smooth. The maximum of plastic deformation is concentrated in the center of the site. The gradient of plastic deformation increases in the direction to the contour, dividing the near-boundary zone. The gradient is maximum at the point on the contour and equal to the value, prescribed by Eq. (25) (Fig. 18).

Equation (29) and the results, presented in Figs. 17 and 18, reveal that with increase in β-parameter the gradients of plastic deformation increase at the distance h from the boundary of the site. Along with it, within the interval $x < a - h$ the region of practically homogeneous plastic deformation arises and expanded. The change in

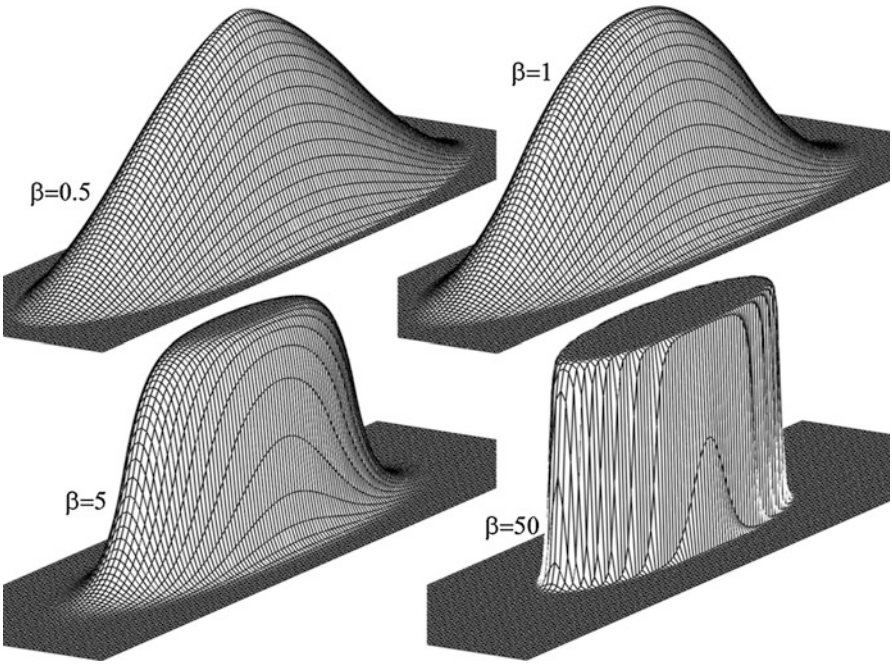

Fig. 17 The changing of the distribution of plastic deformation ε_y in the site of elliptical shape with increase in parameter β in Eq. (29)

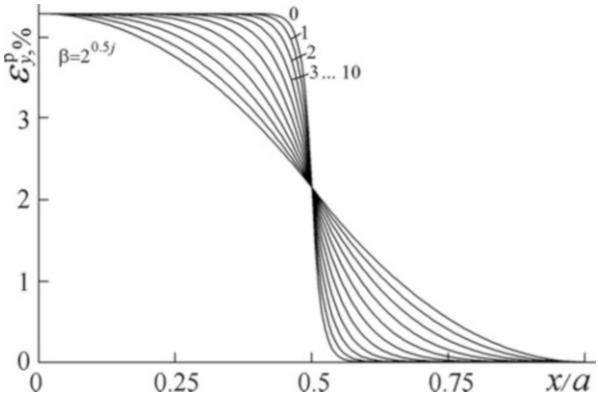

Fig. 18 The changing of the profile of plastic deformation along x axis according to the Eq. (6.10) when β increases by law $\beta = 2^{0.5j}$ (j = 0, 1, 2, 3, . . . 10). $h/a = 0.5$

the width of the near-boundary zone h doesn't influence the maximum gradient, but reduce the area of homogeneous plastic deformation inside the site (Fig. 19).

Qualitative pattern of the distribution of the component ε_x apparently will be analogous to the distributions considered, i.e., the Eq. (21) for $d\varepsilon_y$ and $d\varepsilon_x$ differ only in the coefficients.

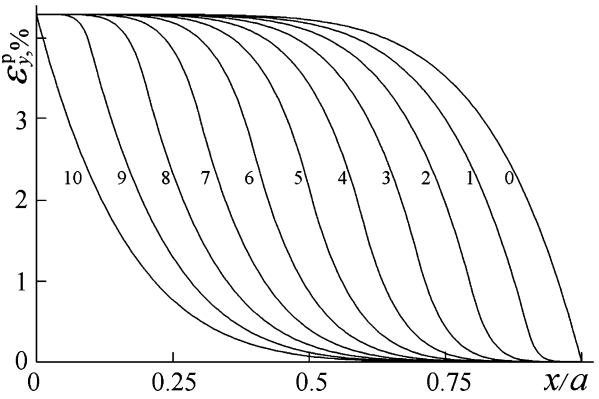

Fig. 19 The change in the profile of plastic deformation along x at h increase from 0 to a. $h/a = 0.5j$

4.4 Field of Stresses from the Site of Elliptical Shape

Since there exists an analytical connection between the tensor of relaxation and plastic deformation then by prescribing the distribution of RE in the local volume, the resulting inhomogeneous stress field is defined automatically, in the whole plane, including the region of relaxation. For the relaxation element in the form of ellipse, the components of tensor of elementary stress field along x-axis can be written in the following form:

$$\begin{aligned} d\sigma_{xx} &= d\sigma^{r}\frac{a}{a-b}\left[\frac{a}{(a-b)}\left(\frac{x}{c}-1\right)-\frac{b^2x}{c^3}\right], \\ d\sigma_{yy} &= d\sigma^{r}\frac{a}{a-b}\left[\frac{b^2}{(a-b)}+\frac{x(a-2b)}{(a-b)c}+\frac{b^2x}{c^3}\right], \\ d\tau_{xy} &= 0. \end{aligned} \tag{30}$$

Here $c = \sqrt{x^2 - \left(a^2 - b^2\right)(1-t)^2}$. The equation for $d\sigma^r$ in Eq. (30) is selected depending on the character of distribution of plastic deformation.

Integrating the Eq. (30) over t variable for the general case of distribution (29) we obtain the distributions, depicted in Fig. 20 depending on the value of the parameter β.

The results of integration for different h values at $\beta = 4$ are represented in Fig. 21 in the form of corresponding profiles of stresses.

A comparison of stress fields with corresponding profiles of plastic deformation immediately reveals a clear correlation. The stress fields have no breaking points (turning points) at $\beta > 0$. Increasing the gradient of plastic deformation (increase in parameter β) causes corresponding growth of the stress gradient, but with the opposite sign. Maximum of the gradients is observed at the points of the contour, separating the near-boundary zone. Besides that, the increase in the average degree of plastic deformation is accompanied by decrease in the stress field inside the site.

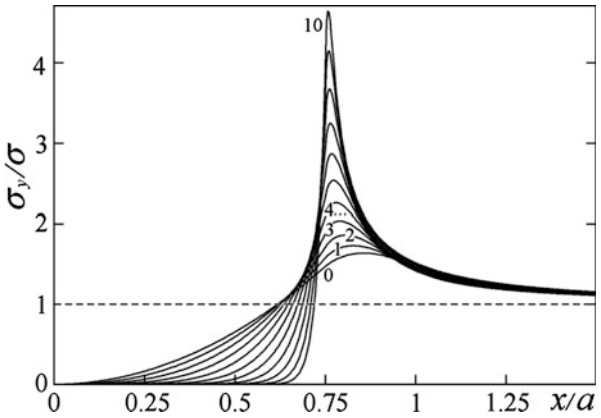

Fig. 20 Profile of σ_y along x-axis under increasing β. $\sigma/E = 4.8 \times 10^{-3}$, $\beta = 2^{0.5 \cdot j}$. Numbers at the curves relate to the corresponding j-values

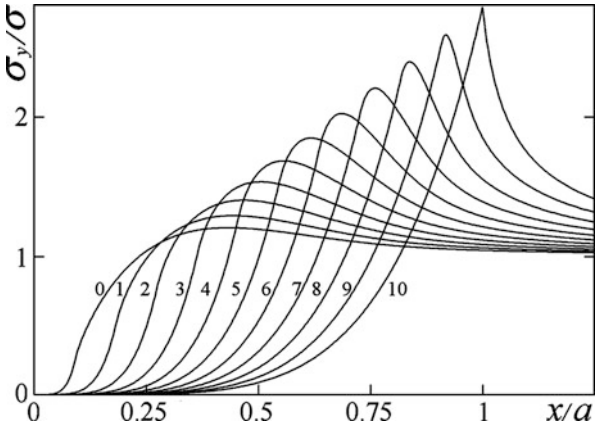

Fig. 21 Changing the profile of stress σ_y along x-axis with increasing h. $\sigma/E = 4.8 \times 10^{-3}$, $h = a \cdot j/11$. The numbers at the curves correspond to j-values

Increase in the width of the near-boundary zone doesn't affect the maximum gradient and results in increase in the average stresses inside the site (Fig. 21).

At the same time within the limits of the width h the stress continuously goes through the maximum. With increase in β-parameter maximum grows. With increase in h an effect of stress concentration wanes, the maximum is smoothing and displacing to the center of the site of plastic deformation. The zone of localized plastic deformation is reduced.

Represented variant of the model of the site of plastic deformation reflects the elastic-plastic properties of real structures in the approximation of continuous medium, when the near-boundary zone is considered to be the physical boundary of the structural elements where the ability to stress relaxation is smoothly decreases as the geometrical boundary with elastically deformed matrix is approached. The results of calculations show that in this case the maximum stress concentration is observed not at the geometrical boundary but in the near-boundary zone with the width not more than h. Increase in the gradients ahead of the physical boundary,

decrease in its width *h,* and the increase in the length of plastic region promote the effect of stress concentration.

5 REM in the Models of Localization of Plastic Deformation and Fracture

5.1 Peculiarities of the Simulation by the Relaxation Element Method

Using the relaxation elements as the defects, characterizing the interrelation between plastic deformation and stress allows one to simulate the process of strain localization and to obtain the dependencies of flow stress on the sequence of the involvements of separate structural elements into plastic deformation. A modelled medium is represented in the form of conglomerate of discrete elements, playing the role of elements of the structure. A structural element with the field of plastic deformation is itself a relaxation element. With a certain degree of accuracy this field can be characterized using the different types of RE, considered above. By placing a definite relaxation element in the element of the structure, we at the same time determine the corresponding change in the field of internal stresses in a solid. In such a way, the interaction of the internal stress fields from the elements of structure, undergone plastic deformation, lies on the basis of the modelling with relaxation element method.

Models developed on the basis of REM operate on principles of cellular automata [40, 41]. The calculation field is divided into a number of cells, playing the roles of elements of structure (for example, grain in polycrystal). Each element of the modelled medium possesses the ability to switch its state by discrete jumps in plastic deformation, prescribed by a definite relaxation element. In such a manner, an element of structure is able to increase discretely the degree of plastic deformation and a stress concentration to affect the stress state of the whole volume of solid. The involvement of the structural elements into plastic deformation is realized by definite transition rule (for example at the moment of achieving of a critical value of shear stress). The interaction of the stress field from different structural elements undergone plastic deformation occurs automatically.

When interpreting the results of a simulation, one should take into account that the stress state of a deformed system is controlled only by incompatible plastic deformation connected with stresses in the volume of a solid. The relaxation elements in the present case play the role of defects, responsible for the field of plastic deformation. However, it was experimentally found that the absolute majority of deformation defects at the stage of developed plastic deformation disappear as a result of annihilation, disappearing at internal interfaces and exposing at the free surface of the solid. The stresses caused by these defects will also disappear. What remains is the corresponding field of plastic deformation, not connected with stresses, which satisfies the compatibility condition. Thus in general case one should not neglect the compatible plastic deformation. The problem lies in the fact that the

compatible plastic deformation cannot be represented by a definite analytical function of coordinates. The same formchanging of the solid can be realized by a number of variants of mass transfer of the material, not influencing the stress field. That means that the relaxation element method can correctly calculate the change of stress fields and plastic deformation, caused by the presence of the defect of plastic nature in the volume of material with time. For the definition of the total plastic deformation, including the contribution from the defects, exposed on the surface of the material, the additional conditions are necessary. They can be formulated when calculating the specific structures, taking the known quantitative data from the experiment. In other words, it is necessary to know the prehistory of the development of plastic deformation.

5.2 Modelling of Localization of Deformation in Polycrystals by RE-Method

Let us consider an example of the simulation of plastic strain localization in polycrystals under loading, using the relaxation element in the form of a circle. In this case we use an approximation, assuming that on the mesolevel each crystallite involved into plastic deformation in the polycrystalline agglomerate can be considered as a relaxation element of round shape.

As a criterion of the crystallite involvement into plastic deformation, serves a critical shear stress τ_{cr} in one of two possible directions which were assigned in each crystallite by the generator of random numbers. The direction imitates the orientation of slip planes in crystallite lattice. The second slip system was directed at an angle of $\pi/3$ with respect to the first one. Let us define the boundary condition by the assumption that the transition of the crystallite from elastic into plastic deformed state occurs at the minimum external applied tensile stress σ. That means that the probability of the involvement into plastic deformation is excluded for all crystallites except only one. According to this condition, a new element with the coordinates (x_n, y_n) transfers into the plastic state under external stress:

$$\sigma_n(x_n, y_n) = \frac{2\left[\tau_{cr} - \sum_{i=1}^{n-1} \Delta\tau(x_i, y_i)\right]}{1 + 2\Delta\tau(x_n, y_n)/\Delta\sigma}, \tag{31}$$

where the sum represents the contribution of all previous REs to the shear stresses.

The contribution of i–RE to the effective shear stress from n-RE is calculated according to the equation

$$\Delta\tau(x_i, y_i) = \left[\Delta\sigma_y^i - \Delta\sigma_x^i\right] \sin\alpha_n \cos\alpha_n + \Delta\sigma_{xy}^i \left[\cos^2\alpha_n - \sin^2\alpha_n\right],$$

where α_n is the angle between the allowed direction and the axis of loading, the components $\Delta\sigma_x{}^i$, $\Delta\sigma_y{}^i$ and $\Delta\sigma_{xy}i$ are calculated, using the Eq. (3) for RE of the round form at the values $\Delta\sigma = 50$ MPa and $\tau_{cr} = 50$ MPa. $\kappa\Delta\sigma_x^i$ The calculation field

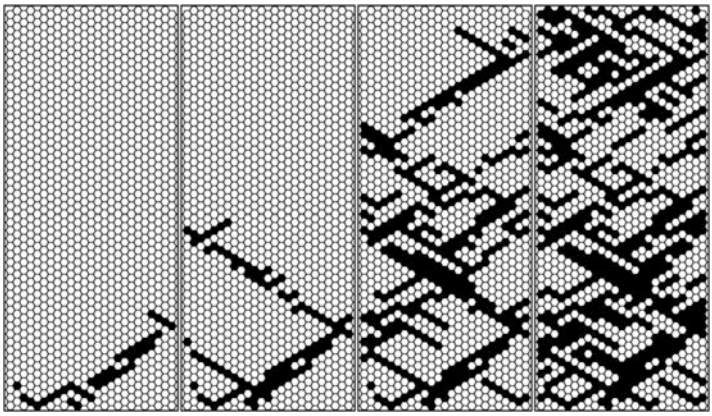

Fig. 22 Self-organization of the bands of localized plastic deformation in the modelled 2D-polycrystal under vertical tensile loading

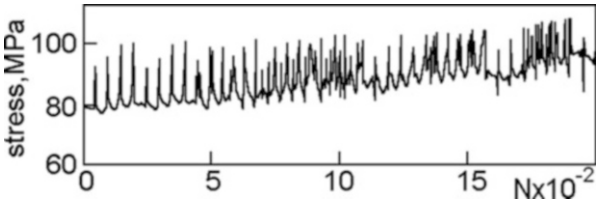

Fig. 23 Dependence of the external stress on the number of crystallites, involved into plastic deformation

consists of 25×50 points – centers of virtual crystallites, which in Fig. 22 are depicted in the form of hexagons.

Shown in Fig. 22 is the sequence of the patterns of the crystallites involvement into plastic deformation. It is seen that under the present conditions, the model predicts the self-organization of the bands of localized shear. From the very beginning of plastic flow, the mesobands divide the material into fragments. The external applied stress oscillates near some average value (31) (Fig. 23). Each stress drop is associated with the formation of a separate mesoband embracing several grains.

A different pattern is observed in the polycrystal with rigid inclusions (Fig. 24). Plastic deformation starts at the boundary of the inclusions and is located near it. The macrobands in the conjugate directions of maximum tangential stresses originate from the inclusion. The contribution of the additional stress fields from the inclusion results into a lower flow stress of the polycrystal. The development of plastic deformation is realized in this case by the formation of mesobands, causing oscillations of the external stress.

Thus, modelling by relaxation element method reveals qualitative and quantitative distinctions of the developments of plastic deformation in polycrystal structures without the inclusion and with a rigid one. The model presented predicts the jump-like dependence of the external stress on the number of acts of structural elements (grains of polycrystals) involvements into plastic deformation. Its value (external

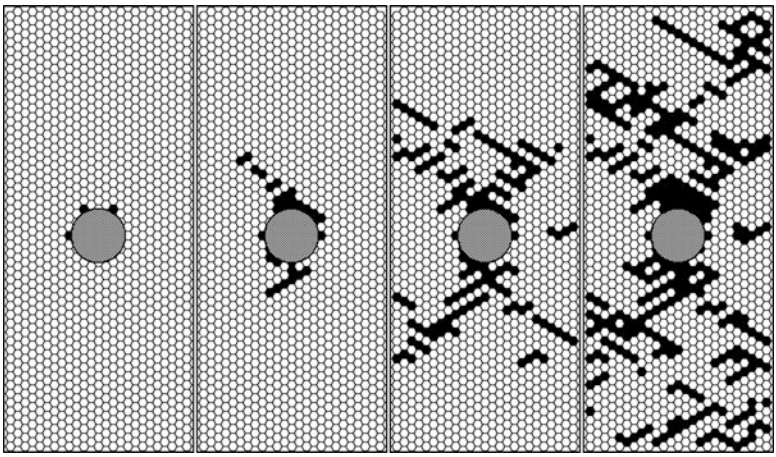

Fig. 24 Self-organization of shear bands in the modelled polycrystal with rigid inclusion

stress) defines the onset of plastic flow in the grain, where a critical value of shear stress is achieved. Since plastic deformation of each new grain changes the field of internal stresses, then the value of external stress oscillates within corresponding limits.

The presented results of the simulation by the relaxation element method points out to the necessity of further improvement of the model. A simplified approach doesn't allow to describe a temporal evolution of strain localization. Besides that, to determine the value of $\sigma(x,y) = \sigma_{\min}$, according to the Eq. (31), practically is not possible. That is why any further improvement of the model of plastic strain localization is realized with accounting of the real boundary condition of loading.

5.3 The Influence of the Rigidity of the Testing Device

Theoretical models of plasticity are developed in assumption of a definite and as a rule simple boundary condition of loading. The changing of the applied load with time is controlled by the change of plastic deformation. It is not possible to realize in practice precise theoretical boundary conditions. Therefore, the loading diagram of the same material depends essentially not only on the mode of loading (tension, compression, bending, torsion), geometrical shape, and the dimension of the specimen but on the technical characteristics of the testing device. One of the most important technical characteristics of the machine is the rigidity modulus M. It is defined as a force which is necessary to apply to the punch of the machine in order to shift in it in 1 mm at the rigid coupling of clamps. Such a displacement is possible due to elastic deformations of the parts of the machine from the punch to the clamp. Depending on the M value the machines conditionally are divided in two classes: into rigid with a big value and into soft with a small value of rigidity modulus. Rigid

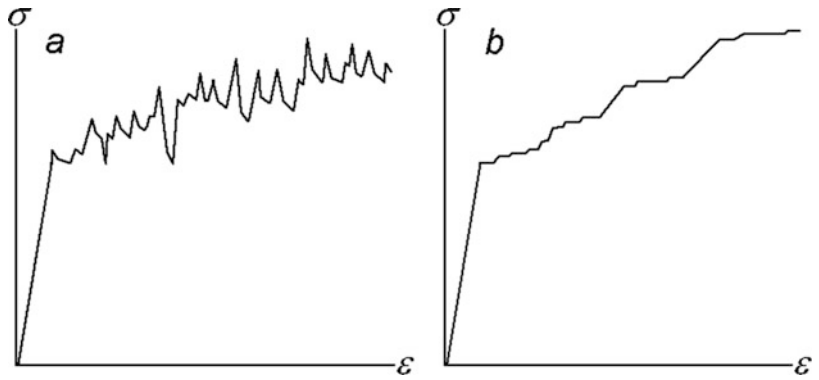

Fig. 25 The view of the loading diagram under tensile loading with application of «rigid» (**a**) and «soft» (**b**) testing

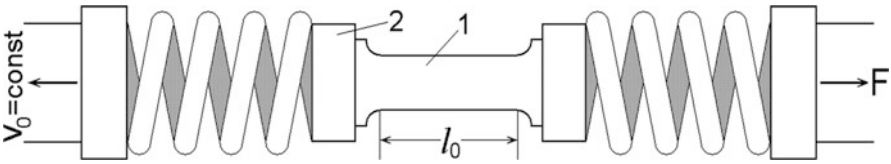

Fig. 26 The scheme: *1* sample, *2* clamp

machines are very sensitive to the quick change in the rate of plastic deformation and react on it by a drop in the load (Fig. 25*a*). The stress-strain diagrams obtained on the soft machine have stair-case type (Fig. 25*b*).

Let the rate of movement of the clamps of testing machine v_0 is known in unloaded state. In the loaded state in a course of deformation of the specimen, the elastic deformation of the intermediate parts of the machine takes place. Therefore a constant change of the strain rate of the specimen occurs. Shown in Fig. 26, the parts of the machine which contribute to elastic displacement are depicted in the form of springs.

According to the definition, the modulus of rigidity of the machine is equal to

$$\mathrm{M} = F/\Delta l_{\mathrm{m}}, \tag{32}$$

where Δl_{m} – is the displacement of the clamps and elastic displacement of the springs. Experimentally, the modulus of rigidity can be defined in the following manner. The clamps of the machine are coupled, excluding the possibility to move with respect to each other. Then the loading is switching on till the nominal magnitude of the force $\mathrm{F_{nom}}$, after which the loading is stopped. Next, it is necessary gradually to uncouple the clamps, to measure the distance Δl_{m} between them and calculate the modulus of rigidity of the machine M, according to Eq. (32).

During the time Δt the punch of the machine will move in a distance $\Delta l^* = v_0 \Delta t$. At the rigid coupled clamps, it will match to the force $\Delta f^* = \mathrm{M}\Delta l^* = v_0 \Delta t$.

If the specimen is deformed in the clamps, then due to the deformation the distance between clamps will increase in

$$\Delta l = [\Delta\varepsilon^{e}(\Delta t) + \Delta\varepsilon^{p}(\Delta t)]l, \tag{33}$$

where l is the effective length of the working part, $\Delta\varepsilon^{e}(\Delta t)$ and $\Delta\varepsilon^{p}(\Delta t)$ – respectively contribution of elastic and plastic deformation of the specimen. In the same length Δl will decrease «the effective length» of the imaginary spring, representing elastic deformation of the intermediate parts of the machine. As a result, the decrease in the force applied to the clamps will take place in a value $\Delta f = \mathrm{M}\ \Delta l$.

The resulting changing of the force will be equal to

$$\Delta F = \Delta f^{*} - \Delta f = \mathrm{M}(\Delta l^{*} - \Delta l) = \mathrm{M}(v_0\Delta t - \Delta l).$$

Then the elastic deformation of the specimen is equal

$$\Delta\varepsilon^{e}(\Delta t) = \Delta F/(\mathrm{S}E), \tag{34}$$

where S – is the area of the cross section of the working part of the specimen and E is Young's modulus.

Plastic deformation of the specimen is equal to $\Delta\varepsilon^{p}(\Delta t) = \dot{\varepsilon}^{p}\Delta t$, where $\dot{\varepsilon}^{p}$ is the average rate of plastic deformation in a prescribed time interval Δt.

Taking into account the equations (33) and (34), we obtain

$$\Delta F(\Delta t) = M\Delta t(v_0 - v^{p})/[1 + \mathrm{M}l/(\mathrm{S}E)]. \tag{35}$$

where v^{p} is the rate of specimen length change due to its plastic deformation.

The sign of $\Delta F(\Delta t)$ depends on the difference of the rates of the punch of the machine and the rate of the change of the length of the specimen due to its plastic deformation v^{p}. At $v^{p} = v_0$ the flow plateau will be observed, and at $v^{p} > v_0$ – decrease in external load. The higher the rigidity of the machine M, the higher is the value of the external drop of the load.

The Portevin–Le Chatelier Effect is connected with periodical spontaneous arising of the band of localized shear. The accumulation of plastic deformation in the band proceeds so effectively, that due to this time the velocity of the increase in the length of the specimen due to its plastic deformation passes ahead the velocity of the movement of the punch of the testing machine. For example, in Al-Al_2O_3 alloys the decrease in external load occurs during 1–2 s. The dependence of the change in external load ΔF (35) in that time interval on the average rate of plastic in the given time interval for the given alloy is presented in Fig. 27. The amplitude of oscillations of external stress at the pointed parameters of the experiments is seen to be 4 MPa if the velocity of plastic deformation of specimen two times passes ahead of the rate of movement of the punch of the machine. Equation (36) can be transformed for the calculation of the increment of external stress $d\sigma$ in time interval dt, during which the stress relaxation in the value $\Delta\sigma$ takes place in the crystallite undergone plastic deformation.

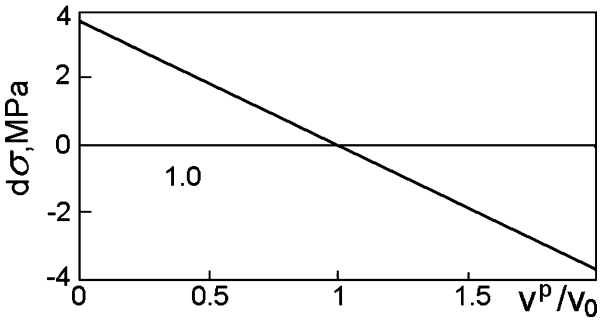

Fig. 27 Dependence of the changing of external load on the relative rate of plastic deformation v^p/v_0: $E = 70$ GPa, $l = 18$ mm, $M = 1.3 \times 10^3$ kN/mm, $\Delta t = 2$ s, $v_0 = 5 \times 10^{-2}$ mm/s

$$d\sigma = \frac{M\left[v_0 dt - Ka^2 \Delta\sigma / bE\right]}{b + Ml_0/(Eh)}. \tag{36}$$

Here, v_0 – is the velocity of the movement of the punch of the machine, a – is the radius of the crystallite, S, l_0, h, and b are the cross section, length, and the width of the working part correspondingly.

5.4 Accounting for Edge Effects

More exact accounting of the boundary conditions of loading in the model is planned to perform because of the following circumstances. The equations represented above for the stress fields are valid for an infinite plane. At that time at the lateral boundaries of the modelled specimen there exist normal and tangential stresses, which should be absent according to the boundary conditions of loading.

Removal of the tangential stresses has been performed, using the method of reflection [42] following the scheme, depicted in Fig. 28. A system of 3 RE is considered, one of which is actual and two others are fictitious. The last create the fields of inverse stresses. The proposed scheme of RE-position practically fully compensates the shear components at the edge of the specimen. It is seen from Fig. 29 that RE causes at the edge of the specimens the components of shear stresses of the significant value (Fig. 29*a*). Application of technique proposed allows easily and simply to compensate for these stresses up to practically negligible values (Fig. 29*b*). At that time, as seen, the stress distribution near the given edge undergoes essential change.

RE causes at the edge of the semi-plane also the normal stresses. For the removal of normal stresses at the edge of the specimen, the following technique has been applied. Fictitious RE, located symmetrically with respect to the boundary of semi-plane increases these stresses twice. This distribution is symmetrical with respect to the line, connecting the centers of the real and imaginary relaxation element.

In mechanics of deformed solid, a problem on the concentrated force applied normally with respect to the surface of isotropic elastic half-plane is known as the Flahman problem [42]. According to the known formula of Flahman, in the system

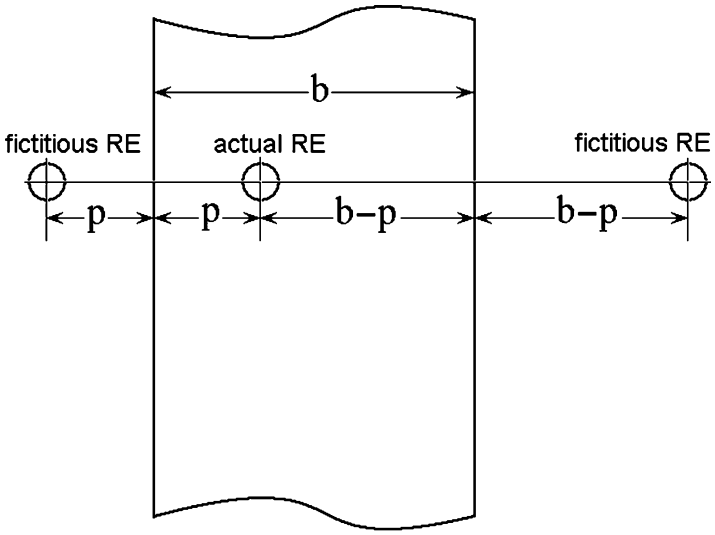

Fig. 28 The scheme of compensation of the shear stresses at the edges of the specimen

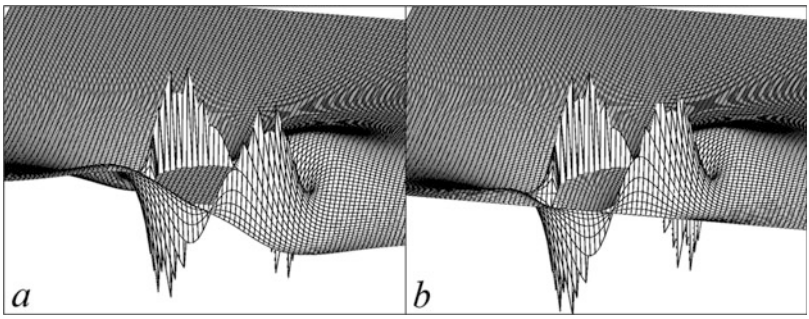

Fig. 29 The distribution of shear stresses in the specimen σ_{xy} before (***a***) and after (***b***) compensation of them at the edge of the specimen

of coordinates, depicted in Fig. 30, under the influence of an elementary force $dF_x = \Delta\sigma_x dl$, operating at the boundary of the half-plane, in the volume of the material the field of stresses with the components arise:

$$d\sigma_x(l) = \frac{2}{\pi}\frac{\Delta\sigma_x(l)x^3}{\left(x^2+l^2\right)^2}dt,\ d\sigma_y(l) = \frac{2}{\pi}\frac{\Delta\sigma_x(l)xl^2}{\left(x^2+l^2\right)^2}dt,$$
$$d\sigma_{xy}(l) = \frac{2}{\pi}\frac{\Delta\sigma_x(l)x^2l}{\left(x^2+l^2\right)^2}dt. \tag{37}$$

Here dl is the elementary segment of the half-plane, in which the stress $\Delta\sigma_x$ operates.

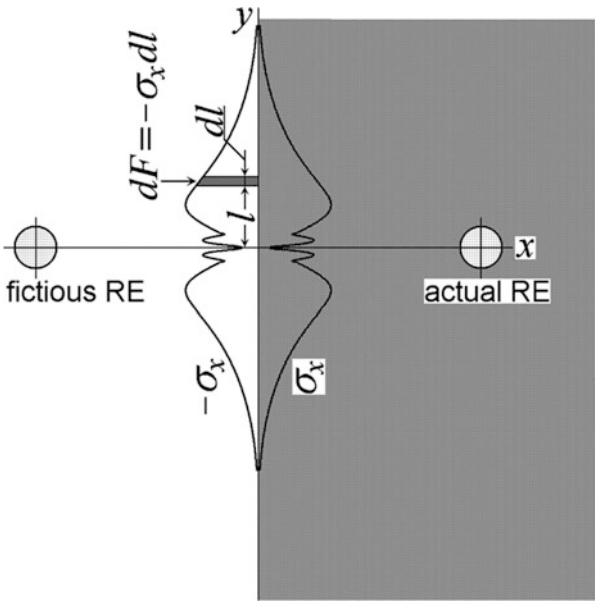

Fig. 30 The scheme of compensation of normal stresses at the edges of the specimen

In order to compensate the normal stresses, created by RE at the edge of half-plane, it is enough to prescribe exactly the same stress distribution in the plane but with the sign reversed. In the system of coordinates in Fig. 30, according to the second equation in the system (38) RE creates the following distribution of normal stresses at $x = 0$, which we will write down with opposite sign:

$$\Delta\sigma_x(l) = \frac{-\Delta\sigma a^2}{\mathrm{p}^2 + t^2}\left(2\left[1 - \frac{2t^2}{\mathrm{p}^2 + t^2}\right] - \left[1 - \frac{8\mathrm{p}^2 t^2}{[\mathrm{p}^2 + t^2]^2}\right]\left(\frac{3a^2}{\mathrm{p}^2 + t^2} - 2\right)\right), \qquad (38)$$

where l is the variable, defining at the edge of the half-plane a location of a specific point in the distribution $\Delta\sigma_x(l)$ (Fig. 30), $\Delta\sigma$ is the value, defining the degree of shear stress relaxation in the RE, and p is the distance from the edge of the specimen till the fictitious RE.

Substitution of the function $\Delta\sigma_x(l)$ in Eq. (37) and their integrations within the limits $-L$ till L, where l is the length of the specimen, defines with enough accuracy the changing of the corresponding components of the stress field in the plane specimen and the compensation of the normal stress at the edge of the specimen. This is very well illustrated in Fig. 31, where the distribution of the normal σ_x stress is represented in the specimen before (a) and after (b) their compensation at the edge of the specimen. It is seen that the approach applied really results in releasing of normal stresses at the edge of the specimen. At that time, an essential changing of the character of distribution takes place.

The technique of the releasing of normal and shear stresses at the edge of the specimen will be further used in modelling.

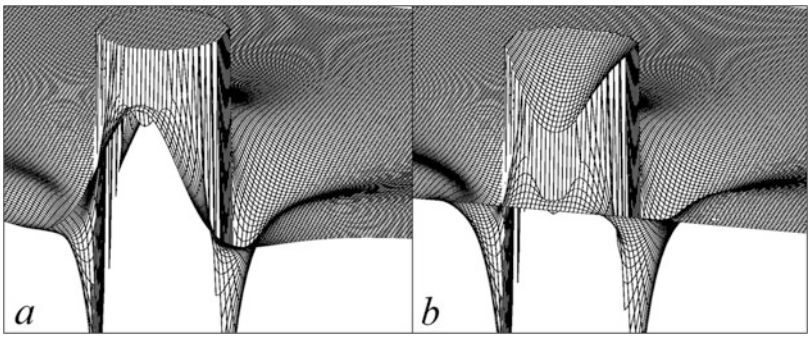

Fig. 31 Distribution of normal stresses σ_x in the specimen before (***a***) and after (***b***) their compensation at the edge of the specimen

5.5 Jump-Like Propagation of the Band of Localized Shear

Equation (8) was put on the basis of algorithm, for the distribution of the stress of pure shear in the conjugate directions at an angle of 45° with respect to the tensile axis without accounting for the different orientations of the slip systems. Such a simplification is justified by the fact that in any case the front of localized shear is usually oriented at an angle of maximum tangential stresses.

This match the case when the crystallites have a large number of slip systems.

The calculation field is represented in the form of a matrix with 10×50 points the centers of crystallite. Onset of plastic deformation was initiated at the edge of the calculation field by placing the RE, represented in Fig. 7 and by Eqs. (14) and (15) at the values $h = 0$ and $\beta = 6$. This grain created a nonhomogeneous field of shear stresses (14) in the volume of the polycrystal. The field of plastic deformation in the crystallite at $h = 0$ is characterized by the tensor with the components

$$\varepsilon_y(x,y) = 2\frac{\Delta\sigma}{E}\left[1 - \left(\frac{r}{a}\right)^{\beta+1}\right], \quad \varepsilon_x(x,y) = -\varepsilon_y(x,y), \quad \varepsilon_{xy}(x,y) = 0. \tag{39}$$

By the formula (31), the minimum external stress was calculated, at which at the center of any crystallite the shear stress achieves its critical value $\tau_{cr} = 50$ MPa. The sum in the numerator defines the contributions from the previous relaxation elements in shear stress. The minimum values of this function correspond to the minimum external stress, at which there is a possibility of involvement of a single crystallite into plastic deformation. The coordinates of the point in which $\sigma = \sigma_{min}$ have been found and a new relaxation element of considered type was put there. In such a manner, such a crystallite possesses a discrete value of plastic deformation (40) and creates around it a corresponding field of internal stresses (14). Thus, the crystallite effects the stress field in the whole volume of solid. The interaction of the fields of internal stresses from the crystallites undergone plastic deformation together with the external applied stress results in the formation of meso- and macrobands of localized plastic deformation.

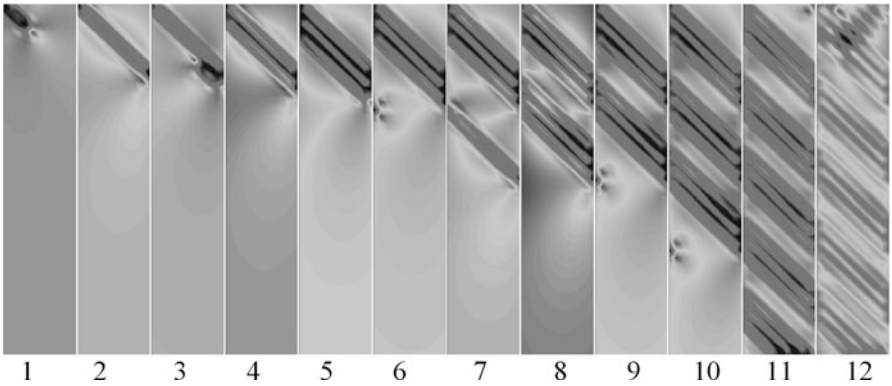

Fig. 32 Consequent formation of meso- and macrobands of localized deformation

Figure 32 illustrates the results of the simulation of the process of strain localization under influence of external applied tensile stress. It is seen that under the operation of the changing inhomogeneous stress field in the volume of the polycrystal a consequent development of the band structure of type B occurs, being typical for a clearly pronounced PLC bands.

The bands of localized plastic deformation, consequently formed as a result of jump-like displacement of the process of strain localization along the working part of the specimen belongs to such type of bands [8]. In the considered case the macroband consists of three mesobands with the width of the diameter of the grain. In front of the formed macroband, a fragment of new mesoband is formed (see the frames 1, 6, 9, 10). It spans over the whole specimen cross section (frames 2, 4, 5, 7) at angle of 45°with respect to tensile axis. The development of the mesoband occurs spontaneously without increasing the external stress. Further the expansion of such mesoband takes place on the mechanism of the front of the Lüders band. (frames 1–5) by consequent involvement of the grains into plastic deformation along the front of initially formed band. A pack (bunch) from three mesobands represents a fully formed macroband (frame 5). At a definite distance from the macroband at the edge of the specimen at that time the zone of increasing shear stresses arises (dark background at the edge of the specimen in the frame 8). Achieving of the critical value of τ_{cr} defines the initiation and development of new macroband of localized shear at the edge of the specimen (frames 6, 9, 10). The process of initiation and propagation of BLD is repeated periodically.

After the process of strain localization achieves the opposite end of the specimen (frame 11), the repeated formation of the macrobands takes place, but already in conjugate direction of the maximum shear stresses (frame 12).

Shown in Fig. 33 is the dependence of external stress on the number of grain involvement into plastic deformation. In fact, this dependence represents by itself a loading diagram of the modelled polycrystal, i.e., each n-act defines a definite quantum of plastic deformation (40).

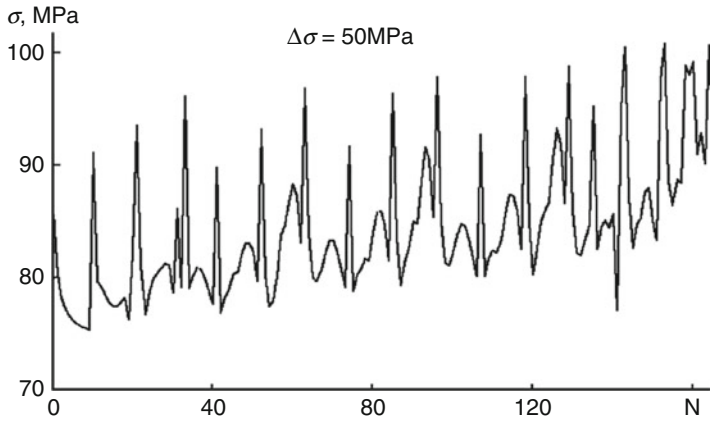

Fig. 33 Effect of interrupted flow at the curve of the dependency of external stress on the number of grains, involved into plastic deformation

Each peak is connected with the initiation of a mesoband of localized deformation at the edge of the specimen. The formation of mesobands occurs spontaneously at the decreasing external stress. The first mesoband from three, composing the macroband requires for its initiation the highest external stresses than others. The lowest external stress corresponds to the initiation of the second mesoband.

In the course of the development of deformation, the onset of the formation of the new BLD occurs at higher external stresses in comparison with the previous band. Thus the change in the field of internal stresses in the chosen mode of intermittent flow results in the effect of work-hardening.

A similar result is obtained for a polycrystal with a noticeably large number of grains (50 × 200) (Fig. 34). Besides the high-frequent oscillations of external stress, here it is observed a long-periodical modulation of stress, connected with arising and formation of new macrobands of localized shear. It is seen that in the process of the formation of the band, work-hardening of the material takes place.

The evolution of the development of strain localization in the modelled polycrystal qualitatively repeats the regularities of the BLD-formation in the alloys with pronounced PLC-effect at the stage of jump-like propagation of the band of localized shear along the working part of the specimen [8, 9].

5.6 Self-Organization of Plastic Deformation in Polycrystals

All the problems of the simulations in mechanics of deformed solid (MDS) is divided into two classes: direct problems (those in which the boundary loading conditions are prescribed and it is necessary to find the stress-strain state) and inverse (stress-strain state is prescribed and it is necessary to define boundary conditions of loading). In MDS there is an actual problem of the solving of inverse problems for

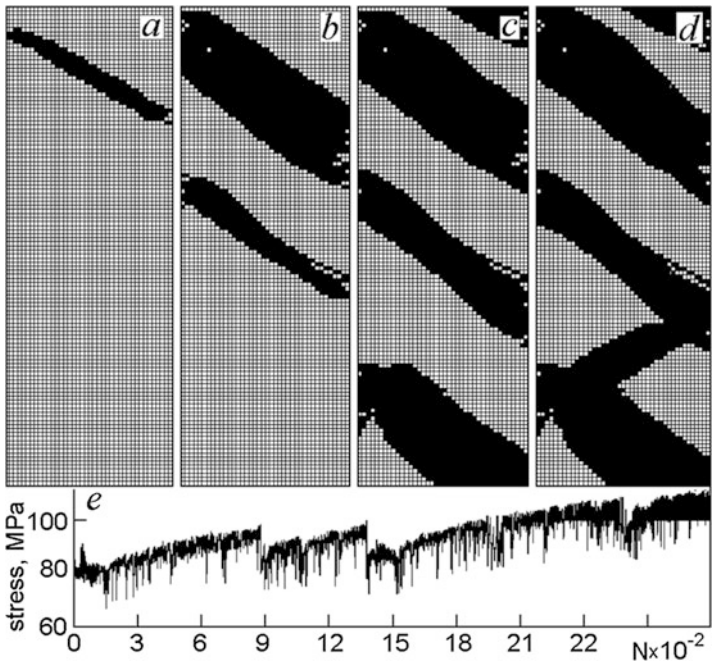

Fig. 34 Jump-like propagation of the process of localized deformation (***a***–***d***)

the case of the plastic deformation in structurally-inhomogeneous media with external and internal interphases.

In the given section, an example of the simulations of self-organization of plastic deformation in polycrystal on mesolevel is given, on the example of the solution of inverse problem of MDS yielding to the macroscopic loading diagrams «σ-ε». A variant of the model in the approximation of plane stress condition of deformed polycrystal is given. On the mesolevel each crystallite involved into plastic deformation is represented as the relaxation element of the round shape. Figure 3 illustrates the perturbation of the homogeneous stress field σ in the volume of polycrystal under the stress relaxation in crystallite in $\Delta\sigma$. The stress concentration of crystallite beyond the crystallite reaches the value $\sigma + 2\Delta\sigma$. The same effect resutls in plastic deformation of the crystallite, characterized by the components $\varepsilon_y^{\mathrm{p}} = 2\Delta\sigma/E$, $\varepsilon_x^{\mathrm{p}} = -\Delta\sigma/E$, $\varepsilon_{xy}^{\mathrm{p}} = 0$, where E is the Young's modulus and $\varepsilon_y^{\mathrm{p}}$ component is directed along the tensile axis.

The onset and development of plastic deformation in a separate grain is assumed to be characterized by two values of shear stress. The first value $\tau_{\max}$ defines the onset of grain involvement into plastic deformation at $\tau_{\max} \geq \tau_{\mathrm{cr}}$, where τ_{cr}, according to the concepts of physical mesomechanics [2–4, 43], is controlled by the processes in grain boundary planar systems. In grain boundaries the movable deformation defects arise and move in the volume of crystallite. In a definite time step dt the relaxation of shear stress occurs in the crystallite till the level τ_0, below

which the plastic deformation in the grain stops. A relaxation measure in the volume of crystallite is defined by the value $\Delta\sigma = 2(\tau_{cr} - \tau_0)$.

The time interval is defined from physical reasoning. For example, the macroband of polycrystals Al-Al_2O_3 with the dimension of crystallite 40 μm contains not less than 4×10^3 grains. The band is formed in 1–2c. Hence, a separate grain is involved into plastic deformation during the time 5×10^{-4} s.

Localization of deformation is developed by the consequent involvement of crystallite into plastic deformation under the operation of concentrators of inhomogeneous field of internal stresses. The involvement of the crystallites into plastic deformation is accompanied by the geometrical formchanging. A force sensor of the test device responds to the change in the length of the specimen. This allows to obtain the dependence of the flow stress on the sequence of separate structural element involvement into plastic deformation. In this way REM allows to realize a transition from the processes of deformation on mesolevel to the loading diagrams of macroscale level.

From the Eq. (37) it is seen that the sign of the increment $d\sigma$ depends on the difference of the rates of velocities of the free movements of the clamps and the rate of change in the specimen length due to plastic deformation v^p. At $v^p = v_0$ a flow plateau is observed, and at $v^p > v_0$ – a decrease in external load. The bigger is the rigidity of the machine M, the more will be the value of drop of the external load.

The equations for the stress fields, derived by REM are valid for the infinite plane. At that time, at the lateral boundaries of the modelled specimen the normal and tangential stresses arise, which should not exist according to the real boundary conditions of loading. During loading these stresses were deleted following the procedure described in 5.4.

The σ-ε was constructed by summation of the increment $d\sigma$, using the obtained Eq. (37).

The effect of rigidity of the tensile testing machine on the loading diagrams of polycrystals of low-carbon steel illustrates Fig. 35 with $E = 210$ GPa [44].

The curve 1 for «soft» mode of loading ($M = 1.3 \times 10^2$ kN/mm) has stair-case type. As the rigidity of the machine M increases from 1.3×10^2 to 1.3×10^8 kN/mm, the curve takes a more saw-tooth shape. The yield drop appears and grows.

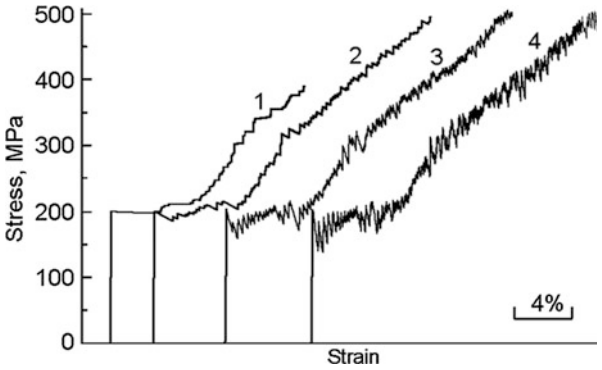

Fig. 35 The effect of the rigidity modulus of the machine M on the type of loading diagramm: M, kN/mm = 1.3×10^2 (1), 1.3×10^3 (2), 1.3×10^5(3), 1.3×10^8(4)

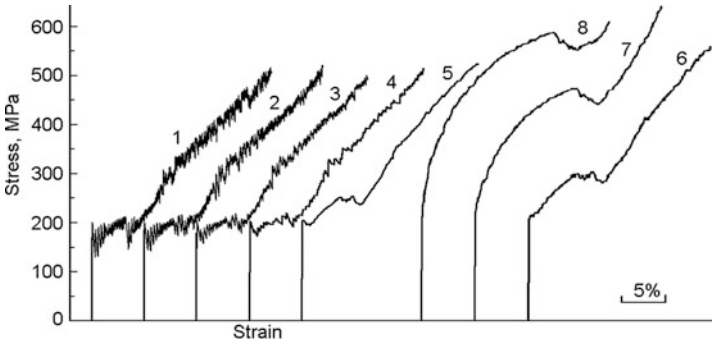

Fig. 36 The effect of the velocity of movement of clamps of loading device v_0 on the shape of loading diagrams: v_0, μm/s = 1 (1), 10 (2), 20 (3), 30 (4), 40 (5), 50 (6), 80 (7), 110 (8)

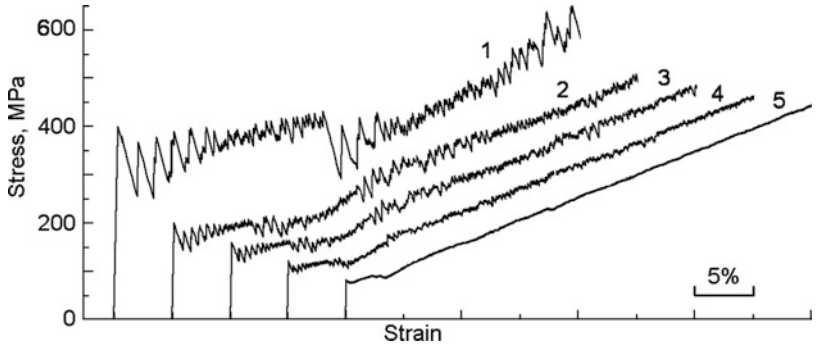

Fig. 37 The influence of τ_{cr} on the loading diagrams:τ_{cr} = 200 (1), 100 (2), 80 (3), 60 (4), 40 (5)

The amplitude of external stress oscillations increases. At all curves the flow plateau is observed, after which the stage of work-hardening follows, caused by internal stress field from relaxation elements. The flow plateau is formed on the mechanism of the Lüders band propagation, when the crystallites is involved into plastic deformation, consequently filling up the working part of the specimen. Repeated involvement of the grains into plastic deformation occurs at higher external applied stresses.

The rate of loading exerts much influence upon the σ–ε curve. The less the rate of loading, the more pronounced is the effect of intermittent flow (Fig. 36). The increase in the loading rate results in a decrease in an amplitude of oscillations of the external curve. Starting from the definite rate of loading there exist no oscillations of external load at the curves (curve 5). A further increase in loading rate results in disappearing of the yield drop and the flow plateau (curves 6–8). The flow stress increases and the effect of a sharp yield stress disappears.

Along with the influence of the rigidity of the machine and the rate of loading, defining the boundary conditions of loading, the effect of the characteristics τ_{cr} of material itself has been considered at the same other parameter of the model. Shown in Fig. 37 are the σ–ε curves for different values of τ_{cr}. If the dislocations are not

blocked by the atoms of admixture (when $\tau_{cr} = \tau_0$), then the phenomenon of intermittent flow is not observed (low curve). As the τ_{cr} increases, the Portevin–Le Chatelier effect arises and enhanced. At that time, the flow stress, flow plateau, and the amplitude of the peaks at the loading diagram increase.

The performed simulations allowed us to reveal qualitative and quantitative changing curves of loading, depending on the characteristics of the material itself and on the boundary conditions of loading. The obtained characteristics of the changes of the qualitative and quantitative loading diagrams when varying the parameters of the model are in agreement with known experimental findings [5–9, 36, 37, 45].

6 The Application of the Relaxation Element Method to the Investigation of the Mechanisms of Plastic Deformation and Fracture

6.1 Stresses of Lüders Band Initiation in Polycrystals

It is known that plastic deformation onset far before the yielding of the material [22, 23, 43]. The grains being exposed on the free surface of the polycrystal are involved into plastic deformation first of all. That is why Lüders band embryo can be represented as the site of plastic deformation at the edge of plane polycrystal. The zone of plastic deformation is assumed to propagate inside the polycrystal at the distance, being equal to the average diameter of polycrystal's grain. For the definiteness let us represent the grain in the form of a proper hexagon. Let the large diagonal of hexagon is directed normal to with respect to tensile y-axis (Fig. 38).

An embryo of Lüders band is represented in the form of a number of relaxation elements enclosed one into another (RE) with the common center and the symmetry axes (Fig. 38). Let us construct the form of the Lüders band embryo in the following manner. The boundary of the embryo, starting from the edge of the polycrystal till the straight line BB′, passes along the half-ellipse's contour with the big half-axes, touching the side of the hexagon in the points B and B′. Further, from the hand-side from the straight line BB′, the boundary passes now along the side of the hexagon till the junction. The slope of the tangent of the ellipse in the points of tangency B and B' is equal to

$$\left|\frac{dy}{dx}\right| = \left[\frac{b}{a}\right]^2 \frac{x_0}{y_0} = \mathrm{tg}\left[\frac{\pi}{3}\right] = \sqrt{3},$$

where b is the small half-axis of the given ellipse. From here we obtain the connection:

$$y_0 = \left[\frac{b}{a}\right]^2 \frac{x_0}{\sqrt{3}}.$$

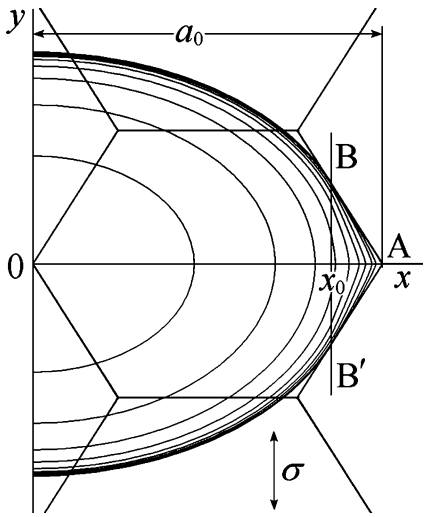

Fig. 38 Scheme of the embryo of the Lüders band at the edge of plane polycrystal

From the other hand, from the equation of the straight line AB it follows that $y_0 = \sqrt{3}(a_0 - x_0)$. By equating these two last formulas, we obtain the following equations:

$$x_0 = \frac{3a^2 a_0}{3a^2 + b^2} \text{ and } \quad y_0 = \frac{\sqrt{3}b^2 a_0}{3a^2 + b^2}. \tag{40}$$

The point with the coordinates (x_0, y_0) belongs to ellipse. Let us present the value of the half-axis of ellipse in the form $a = \mathrm{f} \cdot a_0$, where a_0 is the distance from the edge of polycrystal to the point A (Fig. 38), f is the coefficient of proportionality. By substitution of the value (40) in the equation of ellipses, we obtain the following equation:

$$b = \sqrt{3\left(a_0^2 - a^2\right)} = a_0\sqrt{3\left(1 - \mathrm{f}^2\right)} \tag{41}$$

For the definiteness let us assume that the radius of curvature of the given half-ellipse at the end of its big half-axis, directed along the x-axis, is equal to the half of the average of the dimension of the grain of the polycrystal. The connection d with the big diagonal of the hexagon a_0 we will define by the condition that the area of this grain in the form of hexagon is equal to the area of hypothetical grain in the form of the round region with diameter d. According to this condition $d = a_0\sqrt{3\sqrt{3}/2\pi}$.

Let us construct with the help of ellipses enclosed in each other the continuous distribution of plastic deformation in the embryo of Lüders band. Let us give to the relaxation elements, not intersecting the straight line BB′ (Fig. 38), the shape of half-ellipses with the same relation of the half-axes, being equal to a/b. Within the interval $0 < x < x_0$ the variable $t = 1 - x/a$ will select from the many RE the

specific contour of the given family. For the simplicity let us assume that the length of the half-axes are equal

$$a(t) = (1-t)dt \text{ and } b(t) = (1-t)dt. \tag{42}$$

Elliptical contours, interacting the straight line BB′, smoothly transforms into hyperbolas with the common center at the junction point A. The value of relaxation for the arbitrary RE from the given distribution we will assign in the form of the function on the variable t:

$$d\sigma = (\beta+1)\sigma(1-t)^{\beta}dt, \qquad -1 \le \beta \le \infty, \tag{43}$$

where σ – is the external applied stress.

It is assumed that before the loading, there were no fields of internal stresses in polycrystal and that the matrix beyond the embryo is deformed elastically and isotropically. From general reasoning it is clear that the maximum stress concentration is expected in the vicinity of the junction A of three grains. The instant of Luders band initiation we will define by critical stress σ_y^{cr}.

According to Saint Venant principle, essential influence of the geometrical shape of the grain boundary on the field of stresses will be essential only in the vicinity of the point A.

Let us show that in the points of contours intersection of the contours of RE with the straight line BB′ the continuous transition of the contours from ellipses to hyperbolas takes place.

Let us find the coordinates of the points of intersection of ellipses with the straight line BB′. According to the equation for ellipses

$$\frac{x(t)^2}{a(t)^2} + \frac{y(t)^2}{b(t)^2} = 1, \tag{44}$$

at $x(t) = x_0$ we will obtain the equation

$$\frac{\mathrm{f}^2}{(1-t)^2} + \frac{y(t)^2}{3a_0^2(1-t)^2\left(1-\mathrm{f}^2\right)} = 1.$$

From here we will find the coordinates of the points of intersection:

$$y(t)^2 = 3a_0^2\left(1-\mathrm{f}^2\right)\left[\left(1-\mathrm{f}^2\right) - t(2-t)\right]. \tag{45}$$

On the other hand, hyperbolas in our system of coordinates will be described by the equation

$$\frac{(a_0 - x(t))^2}{a_{\mathrm{r}}(t)^2} - \frac{y(t)^2}{b_{\mathrm{r}}(t)^2} = 1. \tag{46}$$

For all the hyperbolas, the relationship of the half-axis is the same and equal to $b_r(t)/a_r(t) = b_g(t)/a_g(t) = \sqrt{3}$.

From here we will find the small half-axis of the hyperbolas:

$$a_r(t) = a_0\sqrt{(1-f^2)t(2-t)}. \tag{47}$$

Differentiation of (46) with accounting of (47) for each value of the variable t gives the equation of the tangential for the hyperbola at the point of intersection with the straight line BB′ (Fig. 38):

$$\frac{dy}{dx} = \frac{\sqrt{3}\cdot\sqrt{1-f^2}}{\sqrt{(1\text{-}t)^2 - f^2}}. \tag{48}$$

By differentiation of Eq. (44), with accounting of the Eqs. (40) and (41), we assure that the tangential line for the arbitrary ellipse in the point of interaction with the straight line BB′ is also described by Eq. (49), i.e., the smooth transition of the contours of ellipses into contours of hyperbolas.

Thus, parameter *t,* changing from 0 to 1, unambiguously defined the location, shape, and the sizes of the local regions of relaxation in the embryo of the Lüders band. Now we have enough parameters, in order by variation of the β-parameter to regulate the gradients of plastic deformation between the grain boundary and to analyze their influence on the stress concentration in the vicinity of triple grain junction. Further we will neglect the edge effects at the free boundary of plane polycrystal and to consider the stress fields for the case of unlimited medium. According to Saint Venant principle, the effect of the latter on the stress concentration in the point A is insignificant. That is why instead of the half-contours at the edge of the half-plane one can consider the symmetric full contours in unlimited plane.

Before prescribing the distribution of plastic deformation, let us divide the embryo into three zones (Fig. 39) according to the different shape of RE. In the zone I there are RE of proper elliptical shape. The contours intersecting the straight line BB′ fit into zone II, after then the elliptical shape transfer into hyperbolic one. Zone III selects the region, where the contours of the given RE have hyperbolic shape (Fig. 39).

Displacements of the contour of RE of elliptical shape as a result of stress drop in it in the value $d\sigma$ provides the homogeneous field of plastic deformation $d\varepsilon_y = d\sigma$ $(1 + 2b/a)$ [14]. With accounting of (43) we obtain the following equation:

$$d\varepsilon_y = (1-t)^{\beta}(1 + 2b/a)dt. \tag{49}$$

Integration of elementary fields (50) within the interval of changing of the variable t from 1 to $1 - (x^2/a^2 - y^2/b^2)$ defines the following distribution in zone I:

$$\varepsilon I_y^p = \frac{\sigma^r}{E}\left(1 + 2\frac{a}{b}\right)\left[f^{\beta+1} - \left(\frac{x^2}{a^2} + \frac{y^2}{b^2}\right)^{(\beta+1)/2}\right]. \tag{50}$$

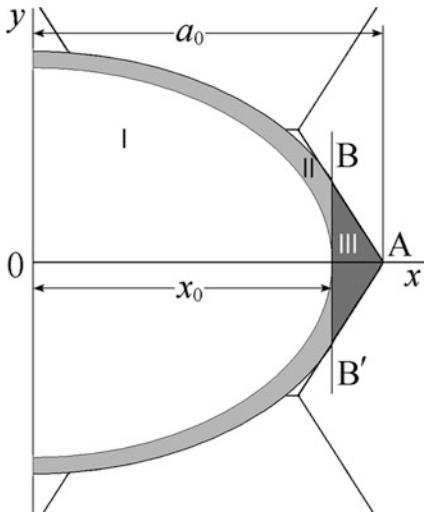

Fig. 39 Zone of plastic deformation in the embryo of a Lüders band

The contribution to plastic deformation from RE not having proper elliptical shape is not possible to define exactly, because there is no exact analytical solution for the displacement of the contour of ellipses, transferring into hyperbola under stress relaxation in it in a definite value. Nevertheless, in simplified variant one can calculate the distribution of plastic deformation in zone II exactly enough.

The results of numerical calculations of the boundary-value problem of the theory of cut-outs reveal, that essential influence on the displacements of the points of the contour and on the stress concentration under tensile loading only two geometrical parameters: the length of the cut-out in the direction normal to tensile axis and the minimum radius of the curvature at the edge of the cut-out along this direction [46–48]. Hence, it is possible to substitute the contour of RE with hyperbolic trajectory at the end of the big semi-axis $a(t)$ with the elliptical contour with the half-axis of the same length and with the radius of the curvature at the end of the band $r(t)$, being equal to those for the corresponding hyperbola. The point displacement of the contour of such an ellipse is easy to define. They will exactly match the displacements of the points of real contour of RE. Then, neglecting the influence of the substitution on the transverse component $d\varepsilon_x^{\mathrm{p}}$, one can easily find an expression

$$\begin{aligned} d\varepsilon_y^{\mathrm{p}} &= \frac{\sigma(\beta+1)}{E}\left\{1+2\sqrt{\frac{a(t)}{r(t)}}\right\}\frac{y'}{y}(1-t)^{\beta}dt \\ &= \frac{\sigma(\beta+1)}{E}\left\{1+\frac{2}{\sqrt{3}}\sqrt{\frac{1}{(1-\mathrm{f}^2)t(2-t)}}\right\}\frac{y'}{y}(1-t)^{\beta}, \end{aligned} \tag{51}$$

where y and y' are the coordinates of corresponding points at the real and substituted contours. $r(t) = [a_0 - a(\mathrm{t})]$ is the curvature radius at the end of the big semi-axis of hyperbola.

Integration of (51) over the variable t with accounting for (44) defines the contributions of RE into plastic deformation, intersecting the straight line BB′. For RE in the Zone II the relationship y'/y is equal

$$(y'/y)_{\text{II}} = \frac{\text{f}\sqrt[4]{t(2-t)}\sqrt{a_0^2\left[1-\sqrt{(1-\text{f}^2)t(2-t)}\right]^2 - x^2}}{\sqrt[4]{1-\text{f}^2}\sqrt{\left[1-\sqrt{(1-\text{f}^2)t(2-t)}\right]\sqrt{a_0^2\text{f}^2(1\text{-}t)^2 - x^2}}},$$

And contribution of distorted RE in the distribution of plastic deformation within the zone II is defined by the equation

$$\varepsilon\text{II}_y^{\text{p}} = \frac{(\beta+1)\sigma^{\text{r}}}{E}\int_0^{1-\sqrt{\frac{x^2}{a^2}+\frac{y^2}{b^2}}}\left[1+\frac{2}{\sqrt{3}}\sqrt{\frac{1}{(1-\text{f}^2)t(2-t)}}\right]\left[\frac{y'}{y}\right]_{\text{II}}(1-t)^{\beta}dt. \quad (52)$$

In zone I at that time will be observed the distribution of plastic deformation $\varepsilon\text{I}_y^{\text{p}*}$, which is defined by the integration of the Eq. (49) from 0 to 1 − f. Thus, in the region, limited by elliptical contour, touching it in the point x_0, this contribution is summed with the component (50).

In the zone III RE contours have the shape of hyperbola. At that time the relationship y'/y is equal

$$(y'/y)_{\text{III}} = \frac{\sqrt{\sqrt{1-\text{f}^2}\sqrt{t(2-t)}}\sqrt{a_0^2\left[1-\sqrt{1-\text{f}^2}\sqrt{t(2-t)}\right]^2 - x^2}}{\sqrt{\left[1-\sqrt{1-\text{f}^2}\sqrt{t(2-t)}\right]\sqrt{(a_0-x)^2 - a_0^2(1-\text{f}^2)t(2-t)}}}.$$

The contribution of RE in the distribution of plastic deformation in the given zone is defined by the equation

$$\varepsilon\text{III}_y^{\text{p}} = \frac{(\beta+1)\sigma^{\text{r}}}{E} \times \int_0^{1-\sqrt{1-\frac{3(a_0-x)^2-y^2}{3a_0(1-\text{f}^2)}}}\left[1+\frac{2}{\sqrt{3}}\sqrt{\frac{1}{(1-\text{f}^2)t(2-t)}}\right]\left[\frac{y'}{y}\right]_{\text{III}}(1-t)^{\beta}dt. \quad (53)$$

The sum of distributions $\varepsilon_y^{\text{p}} = \varepsilon\text{I}_y^{\text{p}} + \varepsilon\text{I}_y^{\text{p}}* + \varepsilon\text{II}_y^{\text{p}} + \varepsilon\text{III}_y^{\text{p}}$ fully describes the distribution of plastic deformation in the nuclei of the Luders band.

Shown in Fig. 40 are the examples of the spatial distributions of plastic deformation in the Lüders band embryo, obtained with the application of the derived above equations. Quantitative and qualitative characteristics of the plastic

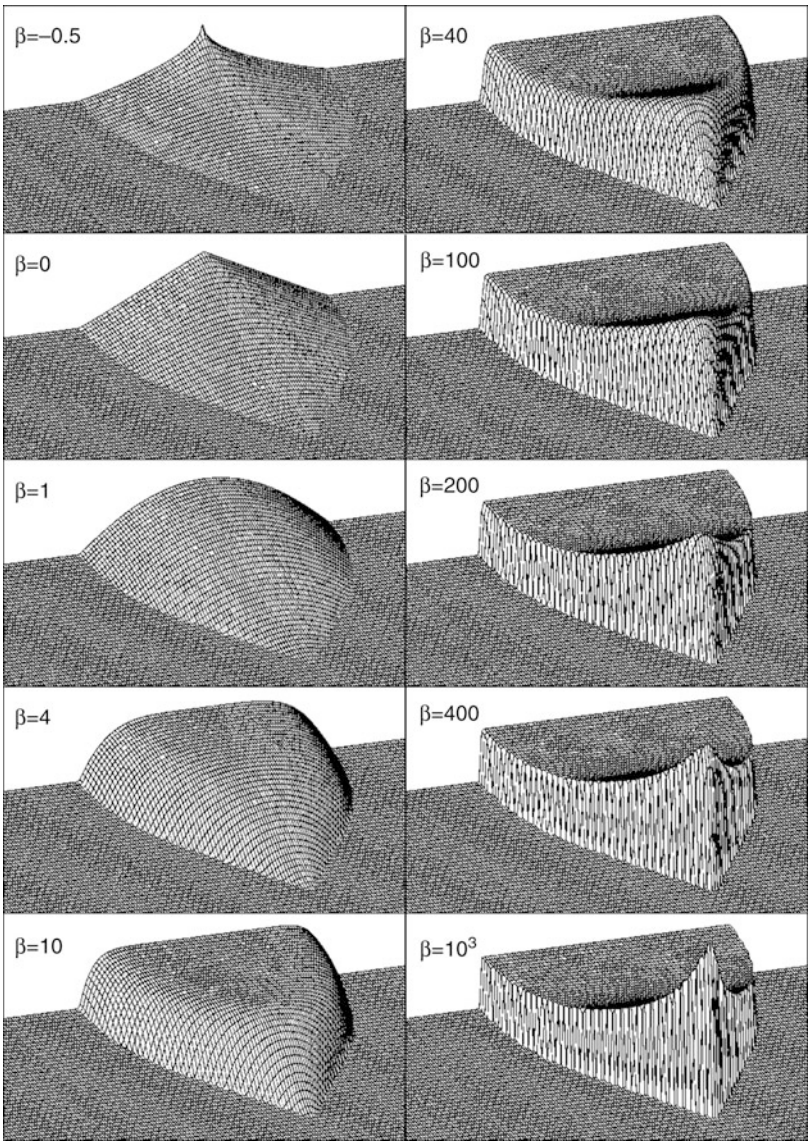

Fig. 40 Examples of the distribution of plastic deformation in the embryo of Lüder's band

deformation distribution depends are seen to depend essentially on the value β-parameter. At increasing β the gradients of plastic deformation at the junction of the embryo increase too. At this time, at a definite instance of time, the zone of elevated concentration of strain arises at the junction. A maximum value of plastic deformation ε_y^p gradually increases, approaching to the junction.

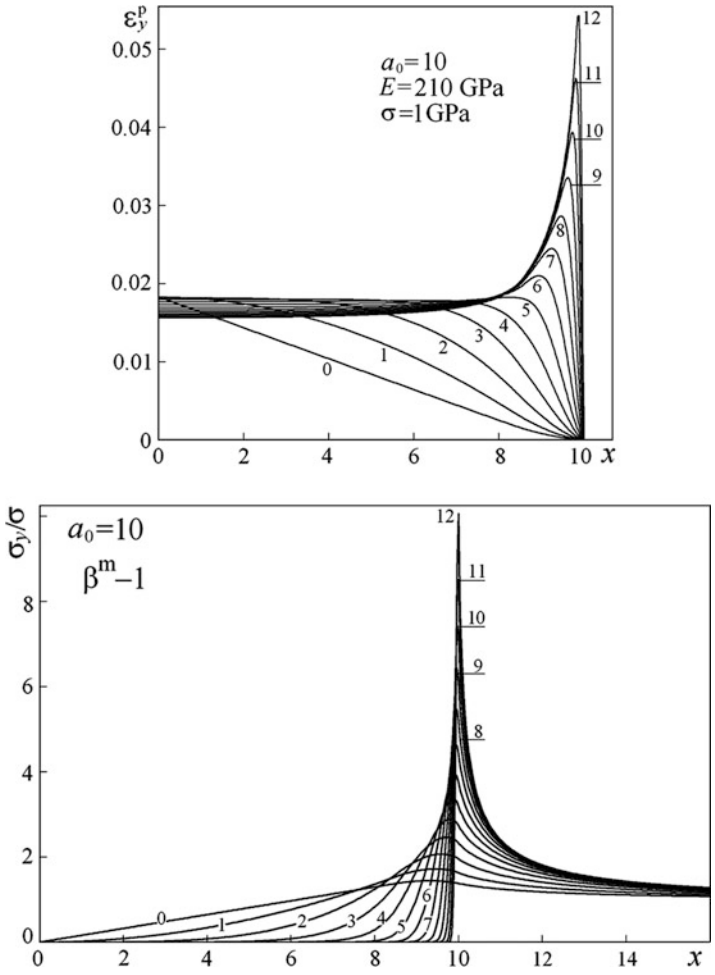

Fig. 41 Profiles of plastic deformation $\varepsilon_y^p(a)$ and stresses $\sigma_y(b)$ along x-axis in the embryo of Lüders band. $\beta = 2^m - 1$. The numbers at the curves indicate m values

The profiles along x-axis of the ε_y^p component for the various values of β are presented in Fig. 41*a*. At the small values of β a smooth decrease of ε_y^p is observed as the junction is approaching. The data are obtained at the value $a_0 = 10$ of the conditional units, $E = 210$ GPa and high external applied stress $\sigma = 1$ GPa. Within creasing β the gradient of plastic deformation at the junction and the maximum is arising and developing, more and more displacing to the junction. At the high gradient the plastic deformation at the junction exceeds the one in the interior of the grain. The calculations show that the contribution of distributions (51) and (53) into plastic deformation at the high values of β-parameter become negligible.

Unfortunately, up to now there is no quantitative experimental data on the distribution of plastic deformation in a separate grain of a polycrystal at the stage of Lüders band initiation. This doesn't allow to define the specific value β, characterizing the degree of heterogeneity of the distribution of plastic deformation for the given material. Nevertheless, given model allows to analyze a stress state of a material in the vicinity of the triple grain junction depending on the gradients of plastic deformation.

About the value of stress state around the embryo one can judge by the profile of the σ_y component along the x-axis.

Stress field from the stress relaxation in the local area in the local value of elliptical shape in the value $\Delta\sigma$ corresponds to the stress distribution for the case of the plane with elliptical cut-out at the uniaxial stress with intensity $\Delta\sigma$. In the latter case the solution is usually given in the elliptical coordinates [49]. The transition to the Cartesian coordinates results to the following equation for the profile of the component σ_y of the stress tensor along x-axis

$$\Delta\sigma_y(x) = \frac{\Delta\sigma a}{a-b}\left[\frac{b^2}{a-b} + \frac{x(a-2b)}{(a-b)c} + \frac{b^2 x}{c^3}\right], \tag{54}$$

where $c = (x^2 - a^2 + b^2)^{1/2}$.

For the arbitrary contour from the family of RE $\Delta\sigma = d\sigma(t)$, with accounting of (42) and (43) the integration of the Eq. (54) will result to the following equation for the σ_y-component along x-axis:

$$\frac{\sigma \mathrm{I}_y}{\sigma} = (\beta+1)\times\int_A^1 \frac{(1-t)^\beta}{a-b} \left[\frac{b^2}{a-b} + \left(\frac{ax(a-2b)}{(a-b)\sqrt{x^2-(a^2-b^2)(1-t)^2}}\right) + \frac{b^2 xa(1-t)^2}{\left(x^2-(a^2-b^2)(1-t)^2\right)^{3/2}}\right]\times dt, \tag{55}$$

where $A = 1 - x/a$ within the interval $0 \le x \le x_0$ and A = 1 − f at $x > x_0$.

For the definition of the contribution to the stress fields from the rest of RE with hyperbolic shape beyond the limits $x > x_0$, i.e., intersecting the straight line BB′, let us use the same Eq. (54), where instead of a and b half-axis of ellipses we substitute the corresponding values a^{f} and b^{f} of half-axis of fictitious ellipses. Radius of curvature of these ellipses at the end of semimajor axis is equal to the radius of curvature of corresponding hyperbolas. By construction, the ratio of semi-axis of all hyperbolas satisfies the equations $b'^2/a'^2 = 3$. From the equations of hyperbolas we can find the distance from the point A to the corresponding hyperbola

$$a'(t) = a_0\sqrt{\left(1-\mathrm{f}^2\right)t(2-t)}.. \tag{56}$$

Hence, the length of the semimajor axis of fictitious ellipses is equal to

$$a^{\mathrm{f}} = a_0\left[1 - a_0\sqrt{\left(1-\mathrm{f}^2\right)t(2-t)}\right] \tag{57}$$

Corresponding radii of curvature at the end of the major half-axis of fictitious ellipses are equal

$$r(t) = 3a^{'} = 3a_0\sqrt{\left(1-\mathrm{f}^2\right)t(2-t)}. \tag{58}$$

The length of the small semi-axis of fictitious ellipses with accounting of (57) and (58) are defined according to the formula

$$b^{\mathrm{f}} = \sqrt{a^{\mathrm{f}}(t)r(t)} = a_0\sqrt{3}\sqrt{1-\sqrt{\left(1-\mathrm{f}^2\right)t(2-t)}}\sqrt[4]{\left(1-\mathrm{f}^2\right)t(2-t)}. \tag{59}$$

Integrating the Eq. (54) within the corresponding limits, where a and b are replaced by a^{f} and b^{f}, correspondingly, we obtain the values σ_y along x-axis. At $x > a_0$ the limits of integration are the same. Within the intervals $x_0 < x < a_0$ limits of integration have the following values, the lower limit is $t_1 = 1 - \mathrm{f}$ and upper limit

$$t_2 = 1 - \sqrt{1 - \frac{1}{1-\mathrm{f}^2}\left[1-\frac{x}{a_0}\right]^2}. \tag{60}$$

The profiles of the components σ_y along x-axes for the different β values are depicted in Fig. 41*b*. It is seen that the stress starting from zero value passes through the maximum near the junction, then falls, asymptotically approaching the level of external applied stress. In the grain interior one can always select the area where the level of σ_y is lower than σ^{r}. With increase in the gradients (β-parameter) stress concentration in the vicinity of junction increases.

The resulting equations define gradient part of stress fields. Besides that, under external applied stress there exist a homogeneous stress field $\sigma_0 = \sigma - \sigma^{\mathrm{r}}$.

At increasing β the maximum σ_y is getting closer to the junction. The area at $\sigma_y < \sigma$ expands. At the high gradients of stress concentration may exceed one order of magnitude and more the external applied stress σ.

In a similar way, one can obtain the equation for the component σ_x. The component σ_{xy} along x-axis is equal to 0.

From general considerations it is clear that stress-strain state in the vicinity of triple grain junction at the moment of Lüders band initiation should not be essentially dependent on the grain size. That means that within the wide range of grain sizes the stress gradients in the vicinity of tripple grain junction should be practically constant. Analysis shows that the maximum (in absolute value) gradient of stress σ_y is always observed in the point of junction A.

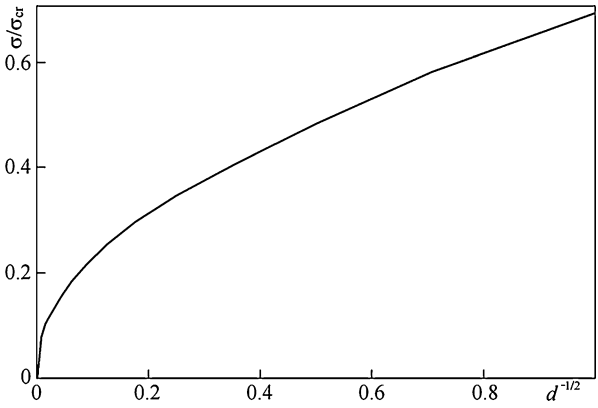

Fig. 42 Stress dependence of the Lüders band initiation on the grain size of polycrystal

From the presented distributions of plastic deformation and stresses it is seen that at the constant values β and σ^{r} with increase in the grain diameter d the gradients of the field decrease under the law of inverse proportionality. In order to fulfill the condition of constancy of the critical stress gradient, it is necessary to decreasing of the gradient to compensate due to the corresponding increase in β parameter and vice versa. To be specific, it is necessary the specific value d_0 (arbitrary unit of grain diameter) to connect with the specific value of β_0 parameter. Shown in Fig. 42 is the dependence of the stress initiation σ'' of the Luders band on the grain size in the embryo at $\tau_{cr} = 1000$ MPa in the coordinates $\sigma'' \approx d^{-1/2}$ at $d_0 = 1$ and $\beta_0 = 0$.

It is seen that with decrease in the grain size the stress of Luders band initiation increases. At $\beta < 1$ σ'' tends to the value of $2\tau_{cr}$ asymptotically. Within a wide range of grain sizes the dependence σ'' on $d^{-1/2}$ obeys almost linear dependence, known as Hall–Petch effect.

Experimental verification of the dependence of flow stress on the grain sizes within a wide interval of d confirms the justice the Hall–Petch law.

In this way, the dependence of mechanical properties of polycrystals on the grain sizes, observed in experiments, is explained by the stress-strain state of the material in the vicinity of the junction of three grains, in which the gradient of plastic deformation plays a principal role. In this connection the attention of experimentalists should be concentrated on the obtaining of the information about the gradients of plastic deformation at the grain boundaries at different stages of loading of structurally inhomogeneous materials.

The method presented extends the possibility on the experiment data to analyze and check the mechanisms, being responsible for the arising and development of plastic flow in the local volumes of corresponding scale. In particular, at the given example of continuum model of Luders band initiation it is shown that specific peculiarities of loading diagrams of real polycrystals are not possible to explain without the accounting of the gradients of plastic deformation in the local volumes and the geometry of elements of structure of the material. At the microconcentrators in structurally inhomogeneous materials, stress concentration can one order of

magnitude exceed the external applied stress. The prediction of the model is very good consistent with the typical regularities, observed in experiments:

- within a wide range of grain sizes the flow stress obeys the Hall–Petch law;
- the average degree of plastic deformation in the grain decreases with decrease in the grain size [50];
- in coarse-grain polycrystals the plastic deformation at the grain junction exceeds essentially those in the interior of the grain [51].

6.2 Modified Model of Crack

The process of the formation of substructures of deformation is often accompanied by the discontinuities and microcracks. In this connection there is an actual problem of the description of the field of stresses at the crack tip [52–54] and the investigation of the influence of plastic deformation of the stress state of solid with crack.

On the basis of the engineering calculations on strength lifetime of the elements of constructions as a rule, the principles and criteria of linear mechanics of fracture are used [52–54]. The latter are obtained, based on the properties of classical model of Griffith crack, in spite of its essential drawback, connected with the presence of singularity at the crack tip, approaching of which results in very quick growth of stress. In this connection in the mechanics of fracture the physical notion of coefficient of stress concentration at the crack tip is not used, but as a characteristic of inhomogeneous stress field a stress intensity factor in the vicinity of singular point is used.

An assumption on the nonlinearity at the crack tips allows to take into account a number of known models for the calculations [55, 56]. However, their application is essentially restricted. They are valid only in the case when the zone of plastic deformation is extremely small in comparison with the length of the crack itself. At the description of the stress state near the crack with significant zone of plastic deformation, there are great mathematical and calculational difficulties.

Critical values of the stress intensity factor K_{Ic} (SIF), characterizing inhomogeneous stress field in the vicinity of crack tip in quasi-brittle material, cannot serve as a parameter, characterizing the ability of the material to resist the crack propagation in metals and alloys, where large plastic deformation precedes the crack nucleation and propagation. That means that the characteristic K_{Ic} for plastic material lose its previous physical sense, especially in the case of testing of small-scaled specimens where the plane strain condition is clearly violated.

It is known that a definite degree of plastic deformation always preceeds the moment of fracture. That means that crack propagation occurs in the layer of plastically deformed material. In other words, the crack from the moment of its nucleation is always surrounded by the layer of plastically deformed material. The thickness of the layer and the distribution of plastic deformation in it apparently depend on the ability of the material to plastic deformation.

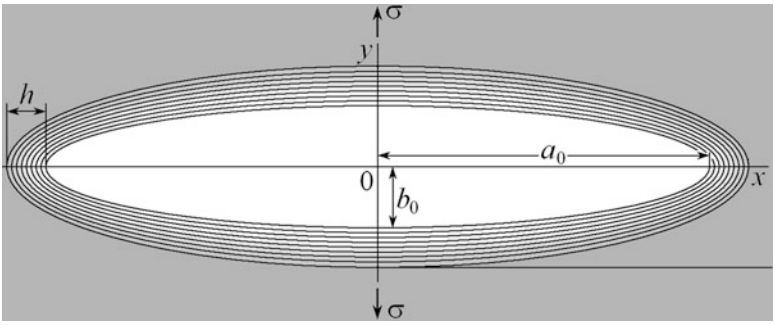

Fig. 43 The scheme of the crack in the surrounding of plastically deformed material

Let us imagine the crack in the form of an elliptical hole with the layer of plastic deformation along the ellipse's contour (Fig. 1). In fact, our task is reduced to the definition of the field of internal stresses of the given system. The continuity condition of material beyond the hole requires smooth changing of stresses from the values in the volume of the material to zero value at the boundary of the hollow. The matrix beyond the selected layer is assumed to be isotropic and is elastically deformed under the operation of tensile stress σ, directed along y-axis. Shown in Fig. 1 is the layer around the crack in the form of relaxation elements of elliptical shape, enclosed in each other. For the definiteness it is necessary to characterize the geometrical parameters of each RE from the family. Let us do it in the following manner. Inside each RE from the given family let us prescribe the value of elementary stress relaxation (elementary stress drop $d\sigma$) in such a manner, that under the external σ an integral sum of stress drop from all the RE eliminates the all stresses in the hollow at the external stress σ (Fig. 43).

Assume that all ellipses have the common center at the origin of coordinates and half-axis coinsiding with the coordinate axis. The length of the semi-axes we define by equations $a(t) = a_0 + h(1-t)$, $b(t) = b_0 + h(1-t)$, where a_0 and b_0 are the big and small semi-axes of the hole, half-axis b of the site is directed along the tensile axis y (Fig. 43), h is the thickness of the length around the hollow, t is the variable, changing within the limits from 0 to 1. At $t = 0$ semi-axes are maximal. Increase in t corresponds to the consequent (gradual) transition from the external ellipses to the geometrical line of the hollow. Specific value t chooses a definite contour from the family. At $b \to 0$ the hollow transforms into a crack. Let $a_0 >> h$, then the point at the axis x corresponds to the RE contour with the variable

$$t = 1 - (x - a_0)/h. \tag{61}$$

The elementary value (infinitely small value) of relaxation tensor for every relaxation element can be written as a function of the variable t:

$$d\sigma_r = (\beta + 1)\sigma t^{\beta} dt, \; -1 \leq \beta \leq \infty. \tag{62}$$

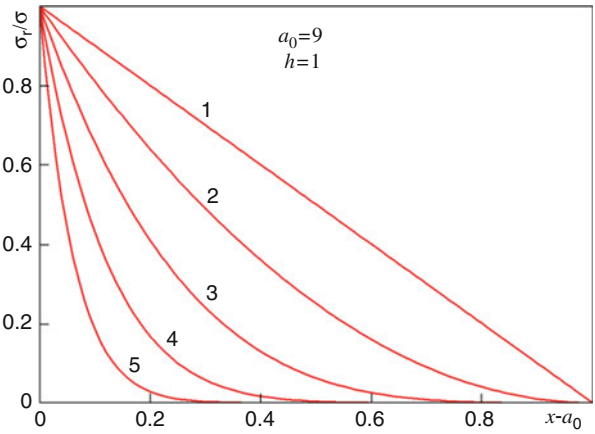

Fig. 44 Normalized relaxation stress in the surface layer for crack with β = 0 (1), 1(2), 3(3), 7(4), 15(5)

The parameter β in the Eq. (62) regulates (controls) the degree of relaxation with continuous transition from one contour to another. Note that the relaxation stress increases with *t*. Superposition holds for the relaxation element as in the linear theory of elasticity. When integrating Eq. (62) from 0 to 1, the normalization factor β+1 ensures inside the hole a full absence of stresses. When integrating Eq. (56) from the value $t = 0$ to the value according to Eq. (61) the value of stress drop increases as the point at the hole is approached. The parameter β regulates the speed of change in the given value. Larger β corresponds to increase in the speed of relaxation. Figure 44 plots the normalized relaxation stress σ_r/σ as a function of distance along *x*-axis within the thickness of the layer. It is seen that the resulting relaxation tensor ensures smooth decrease in the value of stress relaxation.

Increase in the rate of stress relaxation (parameter β) results in the fact that a significant stress drop starts at small distances from the crack tip. In other words, increase in β results in the effect of decrease of physical width of the zone of plastic deformation. Since there is an analytical connection between the elementary relaxation tensor inside and elementary stress field outside [11–14], then by prescribing with the help of the distribution of RE the value of relaxation in the local regions, a resulting inhomogeneous stress field in the whole plane as well as in the layer itself is defined automatically. In the system of coordinates, depicted in Fig. 43, for the components of elementary stress field of arbitrary RE along the *x*-axis, according to conditions (61) and (62), the following equations can be written:

$$d\sigma_{xx} = \sigma(\beta+1)t^{\beta}\left[\left(\frac{x}{\sqrt{x^2-a_0^2}}-1\right)-\frac{h^2(1-t)^2x}{\left(x^2-a_0^2\right)^{3/2}}\right]dt, \tag{63}$$

$$d\sigma_{yy} = \sigma(\beta+1)t^{\beta}\left[\frac{h^2(1-t)^2}{a_0^2}+\frac{x}{\sqrt{x^2-a_0^2}}+\frac{h^2(1-t)^2x}{\left(x^2-a_0^2\right)^{3/2}}\right]dt.,\ d\tau_{xy}=0.$$

In equation the small semi-axis (64) of arbitrary ЭР in the family is equal to $b = h(1 - t)$, as the hollow transfer to the crack at $b_0 = 0$.

By integrating Eq. (63) on the variable t, it is necessary to take into account that beyond the layer the limits of integration are taken from 0 to 1, and at the points, fit in the layer from t to $t = 1 - (x - a_0)/h$. For the profiles of the σ_y component along the x-axes we obtain the following equations:

$$\frac{\sigma_y}{\sigma} = \frac{2h^2}{(\beta+2)(\beta+3)}\left(\frac{1}{a_0^2} + \frac{x}{(x^2 - a_0^2)^{3/2}}\right) + \frac{x}{\sqrt{x^2 - a_0^2}} = A(x), \text{if } x \geq a_0 + h \text{ and}$$

$$\frac{\sigma_y}{\sigma} = A(x)\left[1 - \left(1 - \frac{x - a_0}{h}\right)^{\beta+1}\right] + \frac{\beta+1}{\beta+3}\left(\frac{h^2}{a_0^2} + \frac{xh^2}{(x^2 - a_0^2)^{3/2}}\right)\left(\frac{\beta+4}{\beta+2} + \frac{x - a_0}{h}\right)\left(1 - \frac{x - a_0}{h}\right), \tag{64}$$

if $a_0 \leq x \leq a_0 + h$.

The changing of the stress distribution σ_y, according to (64), at the variation of β-parameter is demonstrated in Fig. 45. It is seen that contrary to the Griffith solution (curve 7), there is no singularity at the crack tip (Fig. 45). Within the surface layer, the stress continuously increases, starting from 0 at the end of the crack, passes through the maximum, then decreases asymptotically approaching the external applied stress σ. Beyond the layer, a qualitative and quantitative discrepancy of the curves is practically disappears. The increase in β parameter results in growth of stress concentration and to the displacement of the maximum towards the boundary of the hollow. In limiting case at $\beta \to \infty$, we yield a Griffith curve (Curve7). The decrease in the physical width h of the surface results in analogous effect (Fig. 46).

The increase in the length of the crack affects greatly the stress concentration (Fig. 47). At that time, contrary to the case in Fig. 46 with increase in the length of

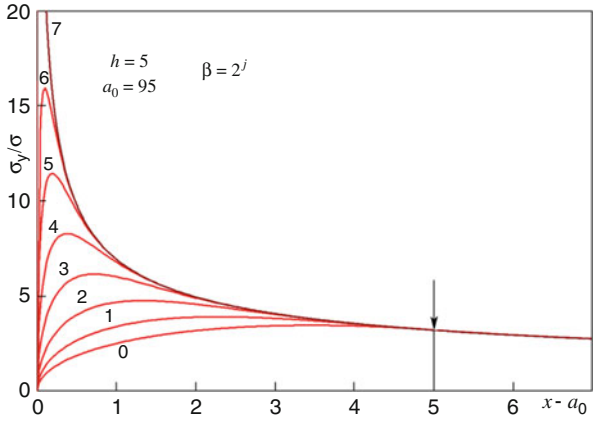

Fig. 45 Profiles of stress σ_y at the crack tip. The numbers at the curves identify the degree of j for $\beta = 2^j$

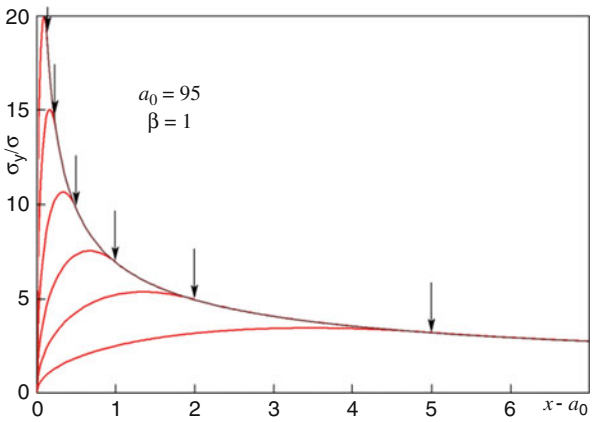

Fig. 46 Profiles σ_y at the crack tip. The arrows indicate the boundary of the zone of plastic deformation

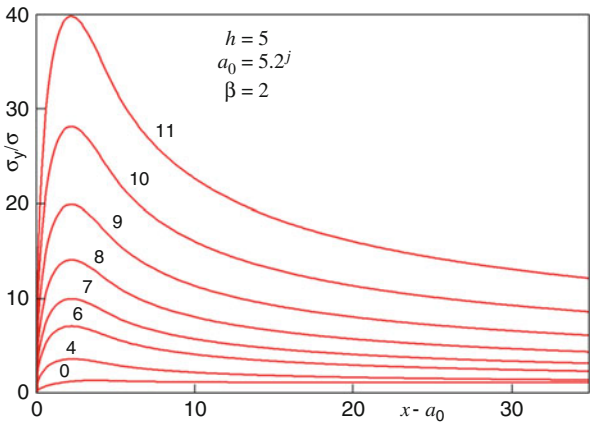

Fig. 47 Profiled of stressσ_y at the crack tip.The numbers at the curves point out the degree of j for $a_0 = 5 \times 2^j$

the crack, the stress increases not only in the near-boundary layer, but also beyond it, i.e., the area of elevated concentration is expanded essentially.

The advantage of the considered description of stress-strain state of solid with crack is apparent, because the singular solution follows from it as a particular case, when the thickness of the layer of plastically deformed material tends to zero, or when the parameter β tends to infinity. The proposed model allows to analyze an effect of the value of the gradient of plastic deformation on the concentration and stress distribution at the crack tip.

7 Conclusion

In this chapter, the possibilities of new methods of the relaxation elements are elucidated. Examples of the construction of sites with gradients of plastic deformation have been given. A stress-strain state of the plane with a round inclusion is

considered. The analytical description of the plane with the band of localized shear is performed.

The possibilities of the modelling by such a method of the effect of the localization of plastic deformation are considered. An analysis of the influence of the rigidity of the testing device on the effect of interrupted flow is presented.

Important results testify to the high predictive possibilities and perspectives of developed method. They are in agreement with known experimental data:

- Effect of intermittent flow is a sequence of the formation of mesobands and macrobands of localized deformation.
- In the changing field of stresses the jump-like propagation of the bands of plastic deformation along the working part of the specimen takes place.
- The increasing of the loading rate suppresses the effect of interrupted.
- A "saw"-type of the σ–ε curve is typical for the rigid mode of loading (device with the a high value of rigidity), in the soft mode of loading σ–ε curves have stair shape.

The following peculiarities of the development of localized deformation have been elucidated:

– The formation of mesobands occurs by the mechanism of the Lüders band propagation and is accompanied by the relaxation of internal stresses.
– The structure of a separate macroband consists of the number of mesobands, being oriented along the direction of maximum tangential stresses.
– Accumulation of the fields of internal stresses in the volume of a polycrystal results in the effect of strain hardening.
– A necessary condition of the arising of Portevin–Le Chatelier effect is the fact that the stress of the onset of plastic deformation of the element of structure is essentially higher than the stress at which the following plastic deformation can proceed. A sufficient condition is the condition at which the velocity of increase in the length of the specimen due to plastic deformation periodically outpaces the velocity of the movement of the clamps of the machine.

References

1. Sutton AP, Balluffi RW. Interfaces in crystalline materials. Oxford: Clarendon Press; 1995.
2. Panin VE. Modern problems of physical mesomechanics. In: Proceedings of the International Conference of MESO-MECHANICS 2000: Role of Mechanics for Development of Science and Technology, June 13–16, 2000, vol. 1. Beijing: Tsinghua University Press; 2000. p. 127–142.
3. Panin VE, Grinyaev YV. Physical mesomechanics – new paradigm at the junction of physics and mechanics. Phys Mesomech. 2003;6(4):9–36.
4. Panin VE, Egorushkin BE, Panin AV. Physical mechanics of deformed solid as multi-level system. Phys Mesomech. 2006;9(3):9–22.
5. Estrin Y, Kubin LP. Spatial coupling and propagative plastic instabilities, Chapter 2. In: Mühlhaus H-B, editor. Continuum models of materials with microstructure. Chichester: John Wiley & Sons Ltd; 1995. p. 395–450.
6. Klose FB, Ziegenbein A, Weidenmüller J, Neuhäuser H, Hähner P. Portevin-Le Chatelier effect in strain and stress controlled tensile tests. Comput Mater Sci. 2003;26:80–6.

7. Zhang Q, Jiang Z, Jiang H, Chen Z, Wu X. On the propagation and pulsation of Portevin-Le Chatelier deformation bands: an experimental study with digital specle pattern metrology. Int J Plast. 2005;21:2150–73.
8. Krishtal MM. Instability and mesoscopic inhomogeneity of plastic deformation. Phys Mesomech. 2004;7(5):5–45.
9. Deryugin YY, Panin VE, Schmauder S, Storozhenko IV. Effects of strain localization in the composites on the basis of Al with Al_2O_3. Phys Mesomech. 2001;4(3):35–47.
10. Deryugin YY. Relaxation Element method. Novosibirsk: Nauka, Siberian publishing House RAN; 1998.
11. Deryugin YY, Lasko GV. Relaxation element method in the problems of mesomechanics and calculations of band structures. In: Panin VE, editor. Physical Mesomechanics and computer-aided design of materials, vol. 1. Novosibirsk: Nauka; 1995. p. 130–61.
12. Deryugin YY, Lasko GV, Schmauder S. Relaxation element method. Comput Mater Sci. 1998;11(3):189–203.
13. Deryugin YY. Relaxation element method in calculations of stress state of elastic plane with the plastic deformation band. Comput Mater Sci. 1999;19:53–68.
14. Deryugin YY, Lasko G, Schmauder S. Relaxation Element Method In Mechanics of Deformed Solid. In: Oster WU, editor. Computational Materials. Hauppauge: Nova Science Publishers, Inc; 2009. p. 479–545.
15. Eshelby JD. Continuum theory of defects. In: Seitz F, Turnbull D, editors. Solid State Physics, vol. 3. New York: Academic Press; 1956. p. 79.
16. de Wit R. (1970) Linear theory of static disclinations. In: Fundamental aspects of dislocation. Ed. by J.A. Simons, R. de Wit, R. Bullough, Nat. Bur. Stand. (US) Spec. Publ. 317, vol. I 651-673.
17. Likhachev VA, Volkov AE, Shudegov VE. Continuum theory of defects. Leningrad: Leningrad University Publishing House; 1986.
18. Rybin VV. Large plastic deformations and damage of metalls. Moscow: Mettallurgia; 1986. 224 p.
19. McHugh PE, Asaro RJ, Sich CF. Cristal plasticity models. In: Suresh S, editor. Fundamental of metal matrix composites. Boston: Butherworth-Heinman; 1993.
20. Harder J. Simulation lokaler Fliessvorgänge in Polykristallen. Braunschweiger Schriften zur Mechanik. B. 28. Braunschweig; 1997.
21. Balokhonov RR, Romanova VA. Numerical simulation of thermo-mechanical behaviour of steels with accounting of Luders band propagation. Appl Mech Tech Phys. 2007;48(5):146–55.
22. Dudarev EF. Microplastic deformation and yield stress of polycrystals. Tomsk: Publishing House of Tomsk University; 1988. 256p.
23. Dudarev EF, Deryugin YeYe. Microplastic deformation and yield stress of polycrystals. Izv Vyzov Fizika. 1982;(6):43–56.
24. Iricibar R, Mazza I, Cabo A. The microscopic strain profile of a propagating. Lüders band front in mild steel. Scr Metall. 1975;9(10):1051–8.
25. Andronov VM, Gvozdikov AM. Stress state at the front of Chernov-Lüders band and unstable plastic flow of crystals. Physica Metals Metallovedenie. 1987;63(6):1212–9.
26. Danilov VI, Zuev LB, Letahova EV, Orlova DV, Ohrimenko IA. Types of localization of plastic deformation and the stages of loading diagrams of metallic materials with different crystalline structure. Appl Mech Tech Phys. 2006;47(2):176–84.
27. Barannikova SA, Danilov VI, Zuev LB. Localization of plastic deformation in mono- and polycrystals of Fe−3%Si –alloy under tension. J Tech Phys. 2004;74(10):52–6.
28. Iricibar R, Mazza I, Cabo A. The microscopic strain profile of a propagating Lüders band front in mild steel. Scr Metall. 1975;9(10):1051–8.
29. Sakui S, Sakai T. The effect of strain rate, temperature and grain size on the lower yield stress and flow stress of pure iron. Proc Int Conf Sci Technol Iron Steel, Tokyo Part 2 Tokyo (1971). 1970:989–91.
30. Bell JF. In: Filin AP, editor. Experimental basis of mechanics of deformed solids. M.: Nauka; 1984. 600 p.
31. Wirtman J, Wirtman JP. Mechanical properties, insignificantly depending on the temperature. In: Han RU, Haasen P-T, editors. Phizicheskoe metallovedenie. Moscow: Metallurgiya; 1987. 663 p.

32. Stress relaxation testing. In: Fox A, editor. Symposium on Mechanical Testing, American Society for Testing and Materials, Kansas City, Mo, 24, 25 May 1978. Philadelphia: American Society for Testing and Materials; 1979. p. 216S.
33. Oding IA, editor. Creep and stress relaxation in metals. Academy of Sciences of the U.S.S.R. All-Union Institute of Scientific and Technical Information. Edinburgh: Oliver & Boyd, X; 1965. p. 377S.
34. Kirsch G. Die Theorie der Elastizitat und die Bedurfnisse der Festigkeitslehre. Zantralblatt: Berlin Deutscher Ingenieure. 1898;42:797–807.
35. Timoshenko SP, Goodier JN. Theory of elasticity. 3rd ed. New York: McGraw Hill; 1970.
36. Ziegenbein A, Plessing, Näuhauser X. Investigation of the mesolevel of deformation at the formation of Luder's band in monocrystals of concentrated alloys on the basis of Iron. Phys Mesomech. 1998;1(2):5–20.
37. Malin A, Hubert J, Hatherley M. The microstructure of rolled copper single crystals. Zs Metallk. 1981;72(5):310–7.
38. Nakayama Y, Morii K. Microstructure and shear band formation in cold single crystals of Al-Mg alloy. Acta Metall. 1987;35(7 (2)):1747–56.
39. Zasimchuk ЕЭ, Markashova LI. 1998. Microbands in nickel monocrystals, deformed by rolling. Kiev: ANUkr SSR, Institute of Metallophysics, Preparing No. 23. 36p.
40. Gould H, Tobochnik Y. An introduction to computer simulation methods. Pt. 2: Application to physical systems. Moscow: Mir; 1990.
41. Smolin AY. Development of the method of movable cellular automata for the simulaton of the deformation and fracture of the media with accounting to their structure. Habilitation Thesis, Томск, 2009, 285 p.
42. Crouch SL, Starfield AM. Boundary element methods in solid mechanics. London: George Allen & Unwin.
43. Panin VE. Physical mesomechanics of the surface layers in solids. 1999;2(6): 5–23.
44. Physical values: handbook. Moscow: Energoatomizdat; 1991.
45. Koneva NA, Kozlov EV. Physical nature of the stages of plastic deformation. Izv Vyzov, Filika. 1990;33(2):89–106.
46. Kelly A. High-strength materials. Moscow: Mir; 1976. 264p.
47. Peterson IV. Stress intensity factors. Moscow: Mir. 1977. 304p.
48. Thompson A. Substructure strengthening mechanisms. Met Trans. 1977;6:833–42.
49. Muskhelishvili NI. Some basic problems of the mathematical theory of elasticity. Moscow: Nauka. 708 p.
50. Utyashev FZ. Compatibility condition of plastic deformation and the ultimate refinement of the grains in metals. Fizika i technika vysokih davlenii. 2010;20(4):10–20.
51. Rybin VV. Regularities of Mesostructures Development in Metals in the Course of Plastic Deformation. Prob Mater Sci. 2003;33(1):9–28.
52. Hertzberg RW. Deformation and fracture mechanics of engineering materials. New York: Wiley; 1976.
53. Broek D. Elementary engineering fracture mechanics. Leiden: Noordhoff; 1974.
54. Stepanova LV. Mathematical methods of fracture mechanics. Moscow: FIZMATLIT; 2009. 336 p.
55. Dugdale DS. Yielding of steel sheets containing slits. J Mech Phys Solids. 1960;8(2):100–8.
56. Slepyan LI. Mechanics of cracks. Leningrad: Sudostroenie; 1990. 296 p.